ARTICLES
https://doi.org/10.1038/s41589-021-00906-3
nature chemical biology

Check for updates

TmcA functions as a lysine 2-hydroxyisobutyryltransferase to regulate transcription

Hanyang Dong[1,2], Yujie Zhao[1], Changfen Bi[3], Yue Han[1], Jianji Zhang[1], Xue Bai[1], Guijin Zhai[1], Hui Zhang[1], Shanshan Tian[1], Deqing Hu[4], Liyan Xu[2] and Kai Zhang[1]✉

Protein lysine 2-hydroxyisobutyrylation (Khib) has recently been shown to play a critical role in the regulation of cellular processes. However, the mechanism and functional consequence of Khib in prokaryotes remain unclear. Here we report that TmcA, an RNA acetyltransferase, functions as a lysine 2-hydroxyisobutyryltransferase in the regulation of transcription. We show that TmcA can effectively catalyze Khib both in vitro and intracellularly, and that R502 is a key site for the Khib catalytic activity of TmcA. Using quantitative proteomics, we identified 467 endogenous candidates targeted by TmcA for Khib in *Escherichia coli*. Interestingly, we demonstrate that TmcA can specifically modulate the DNA-binding activity of H-NS, a nucleoid-associated protein, by catalysis of Khib at K121. Furthermore, this TmcA-targeted Khib regulates transcription of acid-resistance genes and enhances *E. coli* survival under acid stress. Our study reveals transcription regulation mediated by TmcA-catalyzed Khib for bacterial acid resistance.

Protein post-translational modification (PTM) plays a critical role in the regulation of diverse cellular processes and disease pathogenesis in eukaryotes[1–7]. As a group of epigenetic marks, histone PTMs are particularly important in the regulation of transcription[8–11]. Despite a lack of histones, nucleoid-associated proteins (NAPs) may perform similar functions in bacteria[12,13]. However, research on the functions of PTMs on NAPs is currently limited. Recent evidence indicates that lysine acetylation and methylation on NAPs may influence bacterial DNA structure[14,15]. Nonetheless, the regulation mechanism and biological influence of NAP PTMs still remain to be explored.

Lysine Khib was originally identified on histones in eukaryotic cells[16]. Recent studies showed that Khib is involved in the regulation of transcription and metabolism, and demonstrated that Rpd3p and Hos3p in *Saccharomyces cerevisiae* and HDAC2 and HDAC3 in human cells serve as the de-2-hydroxyisobutyrylases while Esa1p in budding yeast and Tip60 and EP300 in human cells function as lysine 2-hydroxyisobutyryltransferases[17–19]. Our recent work demonstrated that Khib exists widely in prokaryotes[20] and that CobB is an extensive lysine de-Khib enzyme that mediates Khib to regulate glycolysis in *Escherichia coli*[21]. Although these findings suggest the biological significance of Khib variability regulated by writer or eraser, the influence of lysine 2-hyroxyisobutyryltransferase in prokaryotes remains unknown and the biological consequences of this catalyzed modification are also unclear.

In this report we demonstrate that TmcA, known as a RNA acetyltransferase, serves as a lysine 2-hydroxyisobutyryltransferase in the regulation of transcription and acid resistance of *E. coli*. We identified TmcA as a 2-hydroxyisobutyryltransferase by screening overexpressed GCN5-related N-acetyltransferase (GNAT) family proteins. We further demonstrate that ATP promotes the 2-hyroxyisobutyryltransferase activity of TmcA and that R502 is a critical site for the catalytic activity of TmcA for Khib. Next, we measured relative differences in Khib levels between wild-type (WT) *E. coli* and the corresponding TmcA knockout (KO) strain using stable isotope labeling by amino acids in cell culture (SILAC)-based quantitative proteomics. We identified 467 endogenous Khib candidates regulated by TmcA. Importantly, we found that TmcA specifically regulates K121hib of H-NS (one of the NAPs) and influences the DNA-binding activity of H-NS. Moreover, overexpression of TmcA or K121hib of H-NS both increased *E. coli* survival under extreme acid stress. Using RNA-sequencing (RNA-seq) and quantitative PCR with reverse transcription (RT–qPCR), we further demonstrate that TmcA can mediate K121hib of H-NS to regulate the transcription of acid-resistance genes and enhance bacterial survival under extreme acid stress. Together, these findings reveal a TmcA-catalyzed Khib function in the regulation of transcription in prokaryotes.

Results

Identification of TmcA as a 2-hydroxyisobutyryltransferase. Because reversible Khib has been implicated in the regulation of biological processes in prokaryotes[21], it is necessary to identify regulatory enzymes of Khib to understand its functions. Our recent work showed that CobB can perform de-Khib in prokaryotes. Meanwhile, because it is known that acetyltransferases (KATs) can catalyze diverse lysine modifications such as acetylation and

[1]The Province and Ministry Co-sponsored Collaborative Innovation Center for Medical Epigenetics, Key Laboratory of Breast Cancer Prevention and Therapy (Ministry of Education), Key Laboratory of Immune Microenvironment and Disease (Ministry of Education), Department of Biochemistry and Molecular Biology, School of Basic Medical Sciences, Tianjin Medical University Cancer Institute and Hospital, Tianjin Medical University General Hospital, Tianjin Medical University, Tianjin, China. [2]The Key Laboratory of Molecular Biology for High Cancer Incidence Coastal Chaoshan Area, Department of Biochemistry and Molecular Biology, Shantou University Medical College, Shantou, China. [3]Tianjin Key Laboratory of Radiation Medicine and Molecular Nuclear Medicine, Institute of Radiation Medicine, Peking Union Medical College & Chinese Academy of Medical Sciences, Tianjin, China. [4]Tianjin Key Laboratory of Medical Epigenetics, Department of Cell Biology, Tianjin Medical University, Tianjin, China. ✉e-mail: kzhang@tmu.edu.cn

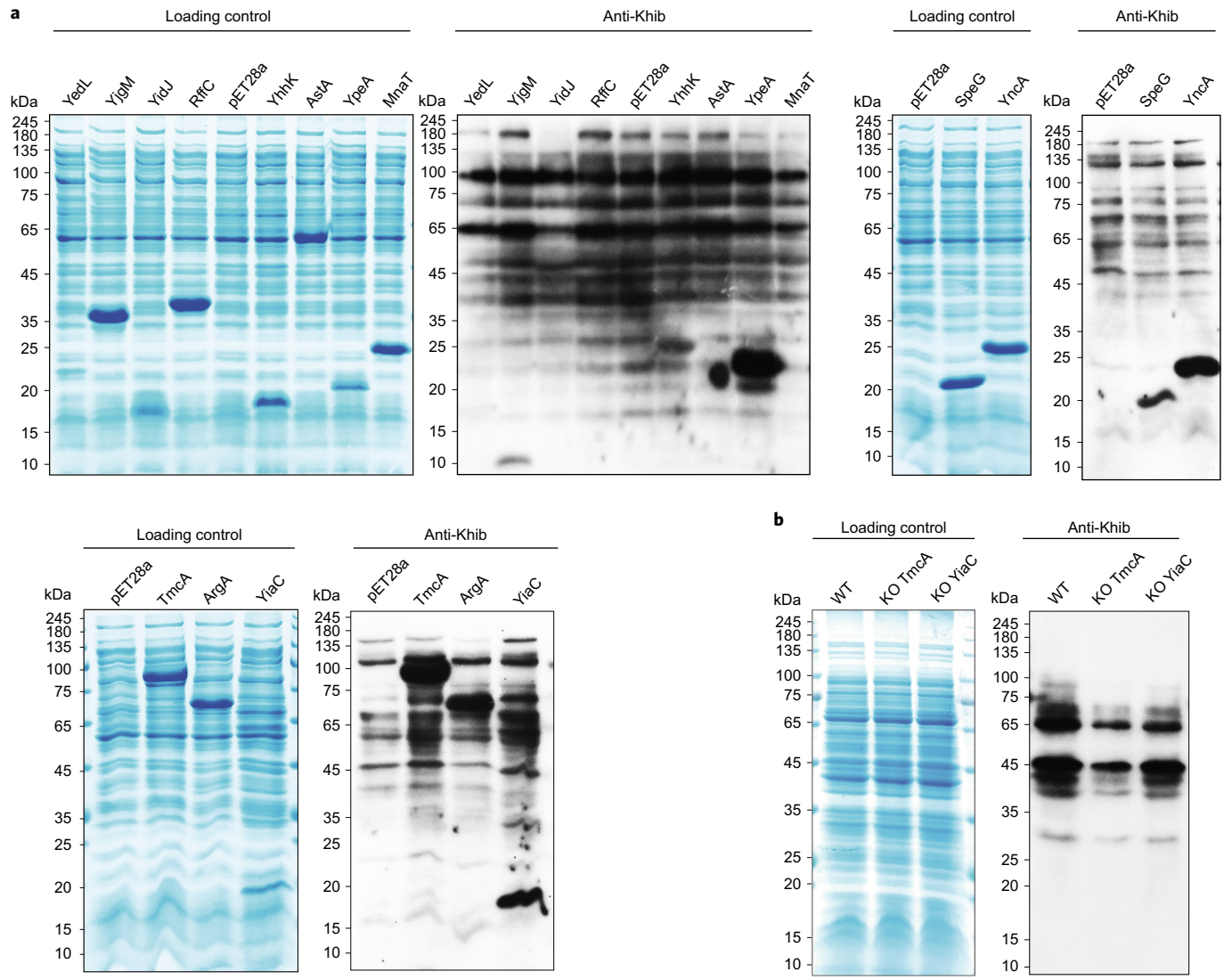

Fig. 1 | Identification of TmcA and YiaC as potential candidates for lysine 2-hyroxyisobutyryltransferase. a, Overexpression of TmcA and YiaC increased Khib levels in *E. coli*. *E. coli* BL21 (DE3) was transferred with an empty vector (pET28a) as control, and with vector GNAT-pET28a for strains overexpressing GNAT; the Khib level of whole-cell lysates was analyzed by immunoblotting. **b**, Deficiency of TmcA or YiaC decreased Khib in *E. coli*. Khib levels of TmcA KO and YiaC KO in *E. coli* MG1655 were analyzed by immunoblotting, with WT as control. All immunoblots had three biological repetitions, with similar results.

succinylation[17,22,23], we reasonably assumed that KATs may also catalyze the addition of Khib in prokaryotes.

Currently, the GNATs are thought to be the only protein family with enzymatic activity for lysine acetylation (Kac) in *E. coli*[24]. To determine whether GNAT proteins can act as lysine 2-hydroxyisobutyryltransferase, we constructed 18 GNAT-overexpressing *E. coli* BL21 (DE3) strains that can stably overexpress GNAT in large quantities (Supplementary Table 2), according to protein sequence conservation[25], and further screened 2-hydroxyisobutyryltransferase by immunoblotting whole-cell lysates with pan-Khib antibody. Compared with WT *E. coli*, we found that strains overexpressing TmcA and YiaC caused an obvious increase in Khib levels whereas overexpression by other strains resulted in no substantial change (Fig. 1a and Extended Data Fig. 1a). Furthermore, we analyzed Khib levels in WT *E. coli* MG1655, YiaC KO and TmcA KO *E. coli* MG1655. Immunoblot assay showed that Khib levels were decreased in YiaC KO and TmcA KO (Fig. 1b), in particular with the latter. Meanwhile, no obvious changes in Kac levels were detected in strains overexpressing TmcA KO or TmcA (Extended Data Fig. 1b,c). Therefore, our results suggest that TmcA and YiaC have a specific impact on intracellular levels of global Khib, and that TmcA is a major candidate for 2-hydroxyisobutyryltransferase.

Arg502 of TmcA is a key site for Khib. A previous study demonstrated that TmcA is a RNA acetyltransferase that catalytically synthesizes N4-acetylcytidine of transfer RNA based on binding with acetyl-CoA[26,27]. Depending on the reported crystal structure of acetyl-CoA-bound TmcA, we decided to test whether TmcA could bind 2-hydroxyisobutyryl-CoA by molecular modeling. We found a difference in binding between acetyl-CoA/TmcA and 2-hydroxyisobutyryl-CoA/TmcA. Structurally, because the 2-hydroxyisobutyryl group can stretch into the catalytic pocket of TmcA (Fig. 2a and Extended Data Fig. 2a,b), it is possible that TmcA possesses catalytic activity toward Khib. To confirm this observation, we synthesized 2-hydroxyisobutyryl-CoA (Supplementary Fig. 1) and expressed TmcA, then performed isothermal titration calorimetry (ITC) assay to detect the binding of TmcA and 2-hydroxyisobutyryl-CoA. As anticipated, there was stronger binding between TmcA and 2-hydroxyisobutyryl-CoA ($K_D = 2.62\,\mu M$)

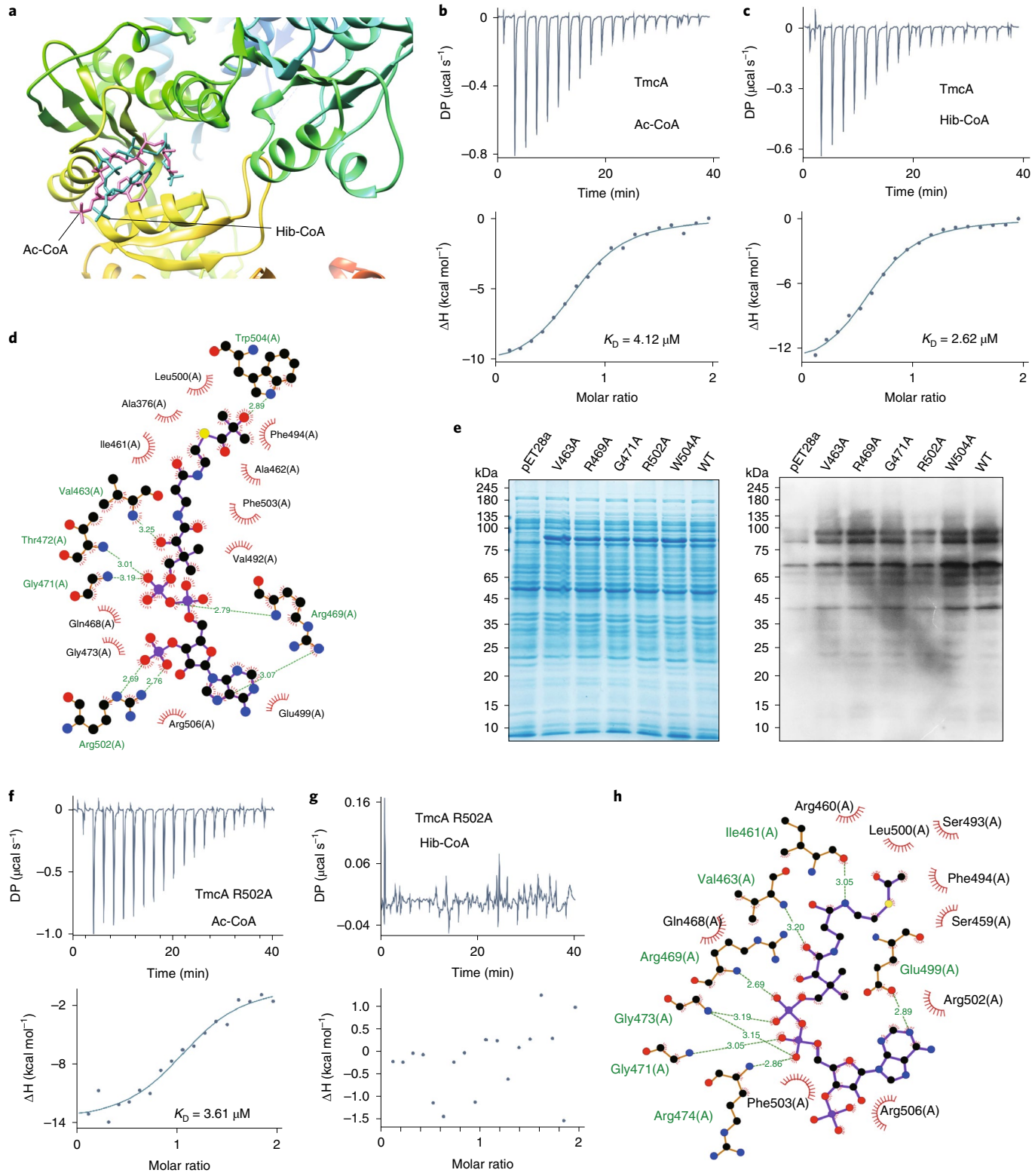

Fig. 2 | R502 of TmcA is a key site for catalysis of Khib by TmcA. a, Structural modeling of TmcA by binding of acetyl-CoA (Ac-CoA) and 2-hyroxyisobutyryl-CoA (Hib-CoA). Crystal structure demonstrated by UCSF Chimera. **b**,**c**, ITC analysis of the affinity of recombinant TmcA with Ac-CoA (**b**) and Hib-CoA (**c**); three biological repetitions, with similar results. **d**, Hydrogen bonds and hydrophobic interactions between TmcA and Hib-CoA from molecular modeling, as shown by LigPlot+, setting the docking box at 100 × 60 × 60 Å. **e**, Khib levels of overexpressing TmcA mutant strains were analyzed by immunoblotting, with transformed strains pET28a and TmcA WT as control; three biological repetitions with similar results. **f**,**g**, ITC analysis of the affinity of recombinant R502A TmcA mutant with Ac-CoA (**f**) and Hib-CoA (**g**); each group had three biological repetitions, with similar results. **h**, Hydrogen bonds and hydrophobic interactions between TmcA and Ac-CoA from crystal structure, as shown by LigPlot+. DP, differential power in ITC assay; ΔH, enthalpy changes.

than between TmcA and acetyl-CoA (K_D = 4.12 μM) (Fig. 2b,c). The ITC results further provide supporting evidence that TmcA can catalyze the addition of Khib.

According to the structural analysis for the binding pocket of TmcA and 2-hydroxyisobutyryl-CoA with the simulation box (100 × 60 × 60 Å), we found six key amino acid residues of TmcA (Val463, Arg469, Gly471, Thr472, Arg502 and Trp504) that can form hydrogen bonds with 2-hydroxyisobutyryl-CoA (Fig. 2d). To highlight the key interacting residues, we zoomed in the simulation box (120 × 80 × 80 Å). Also, we found six similar key residues (Val463, Arg469, Gly471, Gly473, Arg502 and Trp504) forming hydrogen bonds with Hib-CoA (Extended Data Fig. 2c,d). To investigate the active sites of TmcA for Khib catalysis, we selected the same key sites in the two simulations, constructed overexpressing TmcA-Val463A, Arg469A, Gly471A, Arg502A and Trp504A mutant *E. coli* BL21 (DE3) strains and used transformed pET28a and TmcA WT as controls. Next, Khib levels of whole-cell lysates from the above cells were detected by immunoblotting with pan-Khib antibody. We found that Khib levels increased significantly in cells overexpressing TmcA WT, V463A, R469A, G471A and W504A compared with those in pET28a cells (control), but were unchanged in R502A-overexpressing cells (Fig. 2e). We thus reasonably inferred that R502 is probably a key residue of TmcA for Khib catalysis. To confirm this, we applied ITC assay to assess the binding of TmcA R502A with Hib-CoA or acetyl-CoA while performing the same assay for W504A as control. We found that the W504A mutation had no obvious effect on binding with either acetyl-CoA (K_D = 5.11 μM; Extended Data Fig. 2e) or Hib-CoA (K_D = 9.91 μM; Extended Data Fig. 2f), and similarly for R502A with acetyl-CoA (K_D = 3.61 μM; Fig. 2f). In contrast the R502A mutation had a significant effect on binding to Hib-CoA, with the affinity interaction almost disappearing (Fig. 2g). Structurally R502 can form a hydrogen bond with Hib-CoA in the binding pocket and thereby it plays a key role in the binding of TmcA and Hib-CoA (Fig. 2h), while it does not have a similar function in binding with acetyl-CoA. This demonstrates why the TmcA R502A mutation altered binding with Hib-CoA but not with acetyl-CoA. Together, these results demonstrate that R502 is a specific key site regulating the 2-hydroxyisobutyryltransferase activity of TmcA.

TmcA has previously been identified as an RNA acetyltransferase that catalyzes N4-acetylcytidine (ac4C) of tRNA. To elucidate the enzymatic properties of TmcA, we examined whether TmcA R502 could affect the enzymatic activity of TmcA in RNA acetylation. We performed liquid chromatography–tandem mass spectrometry (LC–MS/MS) to detect total ac4C levels in *E. coli* MG1655, and found that ac4C levels in TmcA KO cells decreased significantly but were significantly increased when pPR322-TmcA or pPR322-R502A TmcA was transformed into TmcA KO cells (Extended Data Fig. 3a). This finding indicated that TmcA R502A has little effect on RNA acetylation activity. To verify this, we further detected ac4C by incubation of the synthesized $tRNA^{Met}$ with TmcA or TmcA R502A. Consistent with this intracellular observation, we observed that both TmcA R502A and TmcA can catalyze the formation of ac4C in vitro (Extended Data Fig. 3b). On the basis of these results, we conclude that the TmcA R502A mutation has little effect on enzymatic activity for ac4C, which is separate from its 2-hydroxyisobutyryltransferase activity.

Endogenous Khib substrates targeted by TmcA in *E. coli*. To identify endogenous substrates 2-hydroxyisobutyrylated by TmcA, we performed quantitative proteomics to evaluate the influence of TmcA gene deletion on the 2-hydroxyisobutyrylome in *E. coli*. To this end, we measured the relative levels of Khib between WT and TmcA KO *E. coli*. Using a high-sensitivity proteomic pipeline that combines SILAC and Khib affinity enrichment with two-dimensional LC–MS/MS (Fig. 3a), we identified 4,351 Khib candidate sites in 827 proteins (Supplementary Table 3). We normalized Khib abundance to the level of corresponding proteins (Fig. 3b) and thus quantified 467 obviously downregulated Khib sites (>twofold decrease) in TmcA KO *E. coli* (Fig. 3c). We show that the 12 Khib peptides in the MS/MS spectrum exhibit most changes in response to TmcA knockout in Supplementary Fig. 2. These downregulated Khib sites are potentially functional candidates targeted by TmcA. Meanwhile, we characterized the influence of TmcA gene deletion on the acetylome in *E. coli* by performing the same experiment. In total we quantified 3,086 Kac sites in 913 proteins but, after normalizion of detected abundances to the levels of their corresponding proteins (Extended Data Fig. 4a), only 11 Kac sites were significantly downregulated in TmcA KO cells (Extended Data Fig. 4b and Supplementary Table 4). These data indicate that TmcA has little effect on lysine acetylation intracellularly. To understand the biological significance of TmcA regulation, we further performed a cellular component and pathway enrichment analysis on Khib proteins targeted by TmcA. The results showed that most are related to transcription and translation (Fig. 3d) and are located in the bacterial cytoplasm (Fig. 3e). Meanwhile, protein–protein interaction networks, according to the Search Tool for the Retrieval of Interacting Genes/Proteins, indicated that endogenous substrates were closely connected, especially transcription-related proteins (Extended Data Fig. 5). This finding suggests that Khib regulated by TmcA may be involved in cellular transcription and translation. Further analysis showed that K121hib of H-NS, a site potentially regulated by TmcA, was significantly downregulated in TmcA KO cells. As reported, H-NS is an important histone-like protein that widely binds to the promoter region for inhibition of transcription to maintain bacterial homeostasis[28]. These findings indicate that TmcA may influence transcription in *E. coli*. Therefore, we next focused on the regulatory function of Khib on H-NS.

Regulation of H-NS K121hib by TmcA in vitro and intracellularly. The protein H-NS has three structural components containing an oligomerization activity region (N-terminal domain), a nucleic-acid-binding activity region (carboxyl-terminal domain) and a flexible linker (Fig. 4a)[29]. Proteomics data showed multiple Khib sites on H-NS, most in the nucleic-acid-binding activity region, but the K121hib level showed an obvious decrease in TmcA KO cells only (Fig. 4a and Supplementary Table 3). To confirm the reliability of the Khib peptides identified, we synthesized three types of Khib peptide, one being H-NS K121hib (K(hib)AMDEQGK). As shown in Extended Data Fig. 6a and Supplementary Fig. 3, the entire MS/MS spectrum of synthetic Khib peptides overlaps almost completely with intracellularly modified peptides, and synthetic peptides were also found to be co-eluted with intracellular peptides by high-performance liquid chromatography (HPLC), confirming the reliability of the H-NS K121hib identified. Conservative analysis showed that H-NS K121hib is conserved in bacteria (Extended Data Fig. 6b), indicating that K121 is probably an important site for an evolutionarily conserved function. To verify whether TmcA can regulate H-NS Khib, we incubated recombinant H-NS and mutants with TmcA. As shown in Fig. 4b, TmcA significantly increased Khib levels in both H-NS and K96Q mutant H-NS, while there was no substantial change in K121Q mutant H-NS. We also incubated recombinant H-NS and mutants with YiaC, but there was little effect on the Khib level of H-NS and mutants (Fig. 4c). These results demonstrate that TmcA can specifically catalyze K121hib of H-NS in vitro. Meanwhile, when TmcA R502A was incubated with H-NS there was little effect on the Khib level of H-NS, revealing that R502 is a specific key site for the 2-hydroxyisobutyryltransferase activity of TmcA in vitro (Fig. 4d). Furthermore, we also incubated TmcA or TmcA R502A with H-NS and acetyl-CoA for 2 or 6 h but did not detect any change in acetylation levels of H-NS (Fig. 4e), showing that TmcA cannot catalyze lysine acetylation of H-NS in vitro.

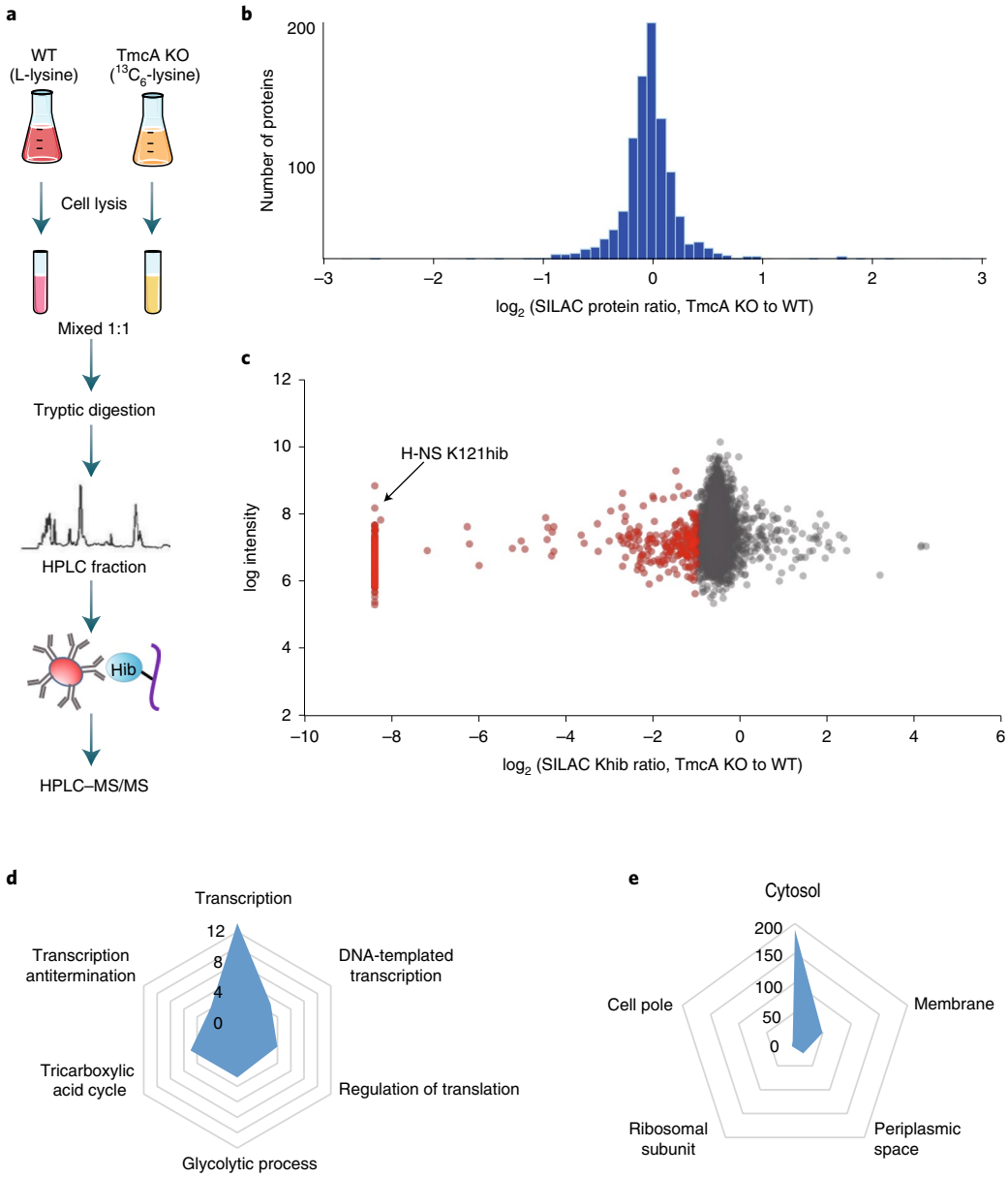

Fig. 3 | Profiling endogenous substrate proteins for Khib by TmcA in *E. coli*. **a**, Schematic representation of experimental workflow for SILAC quantification of Khib in WT and TmcA KO *E. coli*. **b**, Histogram showing relative protein abundance distribution between TmcA KO and WT *E. coli* cells. **c**, Scatterplot showing the ratio of Khib peptides in TmcA KO versus WT *E. coli* cells (normalized by protein abundance). **d**, Biological processes enriched in TmcA-regulated Khib proteomes. **e**, Cellular components enriched in TmcA-regulated Khib proteomes.

To confirm this result intracellularly, a parallel reaction monitoring (PRM) MS assay was performed to detect Khib levels at various Khib sites of H-NS on WT, TmcA KO and YiaC KO *E. coli*, while detecting the peptide of TmcA (LEVVVNER) for normalization. Compared to those in WT cells, Khib levels at various sites were similar in YiaC KO cells but were significantly decreased in TmcA KO cells (while other Khib sites showed no obvious change; Fig. 4f and Supplementary Table 5). In addition, H-NS K121ac was detected only in KO CobB (a lysine deacetylase) *E. coli* and was undetectable in WT *E. coli*[30–32]. Thus finding suggests that H-NS K121ac is of very low abundance compared to H-NS K121hib, and that Khib is the major modification at this site. To test this hypothesis, PRM was further performed and showed that no H-NS K121ac could be detected in *E. coli* MG1655 (Fig. 4g). These results demonstrate that TmcA can specifically catalyze K121hib of H-NS intracellularly.

ATP promotes enzymatic activity of TmcA for Khib. As reported, the RNA acetyltransferase activity of TmcA is driven by ATP hydrolysis. To explore whether ATP hydrolysis is essential for lysine 2-hydroxyisobutyryltransferase of TmcA, purified R319A TmcA was incubated with H-NS, where R319 was reported as a key ATP binding site of TmcA[27]. Immunoblot assay showed that R319A TmcA has no 2-hydroxyisobutyryltransferase activity; meanwhile, we found that TmcA could not increase Khib of H-NS in the absence of ATP after incubation for 2 h (Fig. 4h). Interestingly, when we extended the reaction time to 6 h, both TmcA and TmcA R319A were found increase the Khib level of H-NS in the absence of ATP (Fig. 4i). These results demonstrate that ATP can significantly promote the catalytic activity of TmcA for the generation of Khib.

H-NS K121hib influences DNA binding. Previous studies showed that the major function of H-NS is extensive binding of DNA to

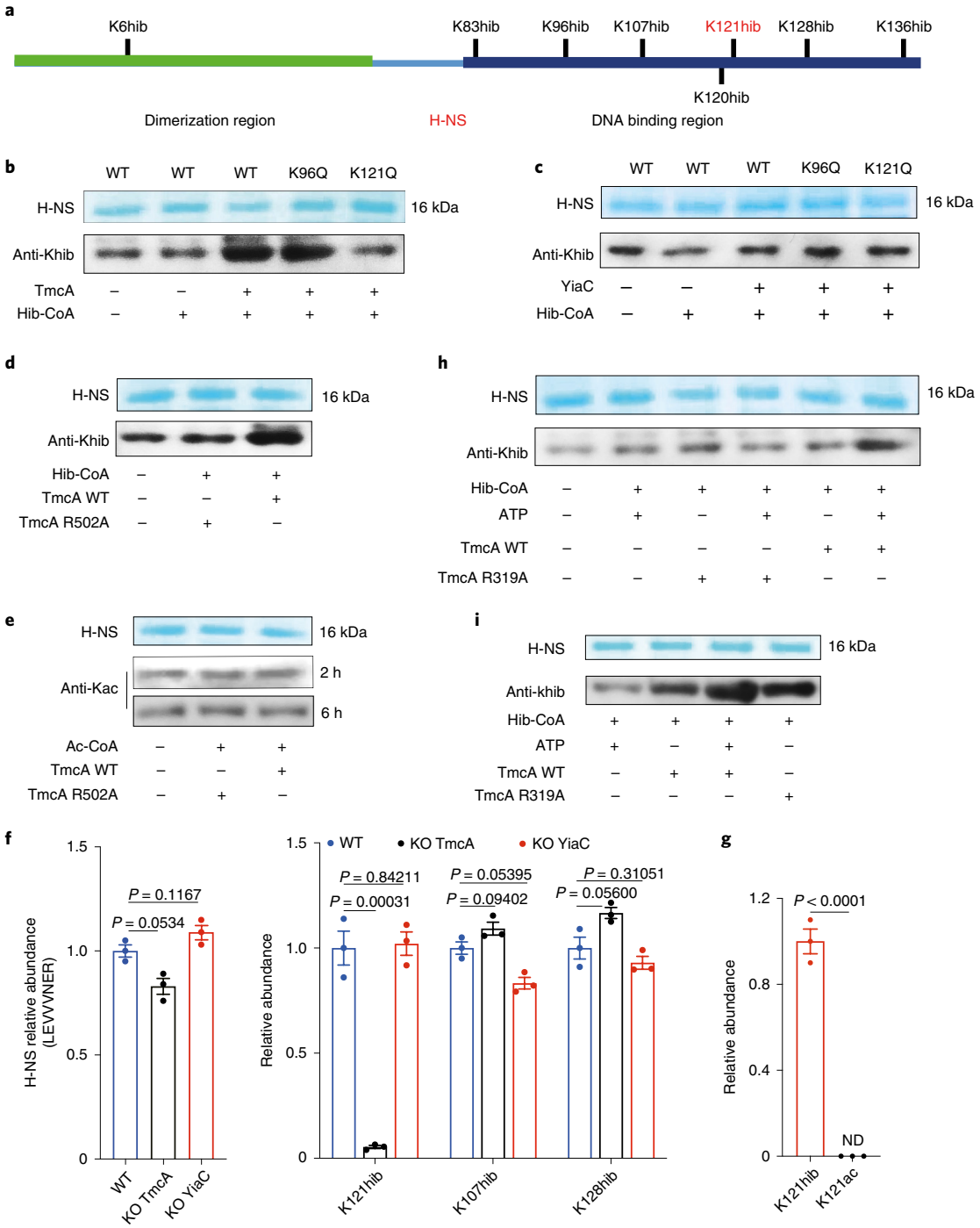

Fig. 4 | TmcA specifically catalyzes K121hib of H-NS. a, Schematic diagram of the structural features of H-NS. **b**,**c**, TmcA can specifically catalyze Khib121 of H-NS in vitro. H-NS or mutant H-NS (K96Q and K121Q) was incubated with TmcA (**b**) or YiaC (**c**) in the presence of Hib-CoA (0.5 mM) for 2 h at 25 °C, and immunoblotting was performed. **d**,**e**, R502 is a key site for catalysis of Khib activity, but not for Kac of TmcA. H-NS was incubated with TmcA or TmcA R502A mutant in the presence of either Hib-CoA (0.5 mM) (**d**) for 2 h or Ac-CoA (0.5 mM) for 2 or 6 h (**e**) at 25 °C, and immunoblotting was performed. **f**, TmcA can specifically catalyze Khib121 of H-NS intracellularly. Comparison of the levels of K107hib, K121hib and K128hib in WT, TmcA KO and YiaC KO strains by PRM assay; each group had three biological repetitions (data presented as mean ± s.e.m., multiple *t*-test, $n = 3$ biological repetitions). **g**, H-NS K121ac level was very low in *E. coli*. Comparison of the quantities of H-NS K121ac and K121hib in WT *E. coli* by PRM assay; each group had three biological repetitions (data presented as mean ± s.e.m.; ND, not detected). **h**,**i**, ATP promotes the 2-hydroxyisobutyryltransferase activity of TmcA. H-NS was incubated with TmcA or TmcA R319A mutant in the presence or absence of ATP (1 mM) for 2 h (**h**) or 6 h (**i**) at 25 °C and immunoblotting was performed. All immunoblotting experiments had three biological repetitions, with similar results.

regulate transcription[28,33]. Because we demonstrated that H-NS K121ac has very low abundance and is not regulated by TmcA, we then focused on the effect of Khib on H-NS K121. Lysine is a basic amino acid with positive charge like arginine (R) but, when K is modified as Khib, the electrical property changes to neutral as for glutamine (Q). To explore the biological significance of H-NS

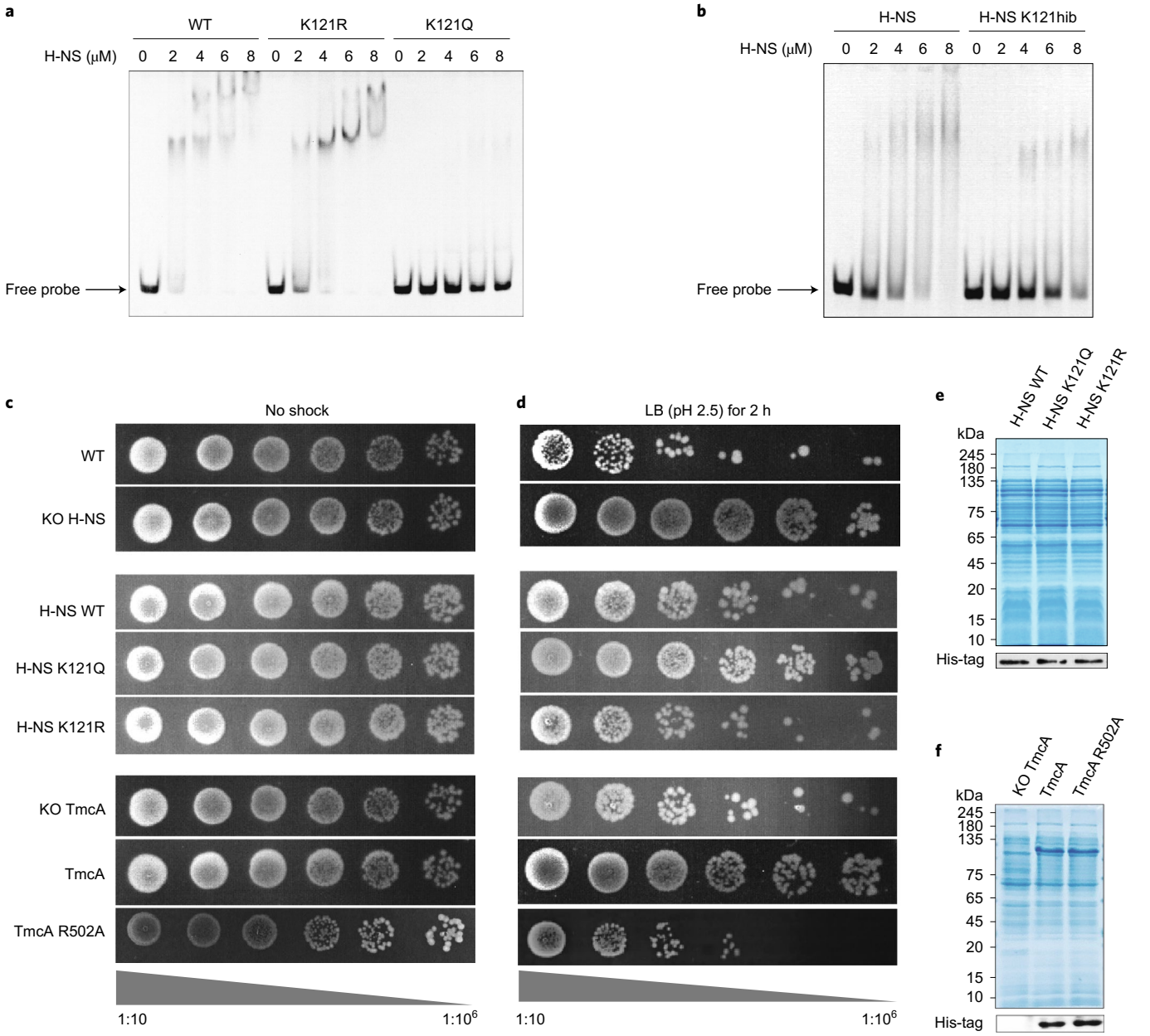

Fig. 5 | TmcA regulates K121hib of H-NS that influences the DNA-binding ability of H-NS and survival under acid stress. a, K121hib of H-NS inhibits H-NS binding with DNA. Equivalent concentrations of H-NS or H-NS mutants were incubated with a DNA probe, and EMSA assay was performed to demonstrate the DNA-binding ability of different H-NS mutants. $n = 3$ biological repetitions. **b**, TmcA regulates K121hib of H-NS that influences the DNA-binding ability of H-NS. H-NS was incubated with TmcA to increase K121hib of H-NS, then modified H-NS was isolated by 50-kDa cutoff tube and incubated with a DNA probe for EMSA assay. $n = 3$ biological repetitions. **c**–**f**, TmcA regulates K121hib of H-NS that influences the survival of strains under acid stress. Survival of strains harboring H-NS mutants following acid shock. Comparison of the viability of WT, H-NS KO and H-NS KO rescued strains harboring H-NS mutants. TmcA KO strain and overexpressing TmcA or TmcA R502A mutant strains were incubated for 1 h in LB medium (**c**) or LB medium acidified by HCl to pH 2.5 (**d**); images represent serial dilutions of cultures in tenfold steps (left to right: 1:1 to 1:10,0000). Immunoblotting was performed to detect expression levels of recombinant TmcA, H-NS and various mutants (**e**,**f**). Immunoblotting and acid stress experiments had three biological repetitions, with similar results.

K121hib, we locked 2-hydroxyisobutyrylated K by Q and unmodified K by R, cloned the *gal* promoter as a probe and, using electrophoretic mobility-shift assay (EMSA), we observed that K121Q mutant H-NS almost lost its DNA-binding activity but the K121R mutant had little effect on binding (Fig. 5a). We also detected other identified Khib sites (K120Q and K128Q), but these had no obvious effect on DNA binding of H-NS (Supplementary Fig. 4). These findings suggest that K121hib can significantly reduce the DNA-binding activity of H-NS. Next, we incubated H-NS with TmcA to increase the K121hib level of H-NS, the modified H-NS being separated by a 50-kDa cutoff centrifugal filter, then performed EMSA; the results showed that K121hib H-NS decreased DNA-binding ability (Fig. 5b), indicating that regulation of H-NS K121hib by TmcA influences the DNA-binding activity of H-NS.

H-NS K121hib enhances the acid resistance of *E. coli*. As reported, H-NS regulated acid stress resistance by silencing the genes related to acid tolerance[34,35]. Our data showed that K121hib

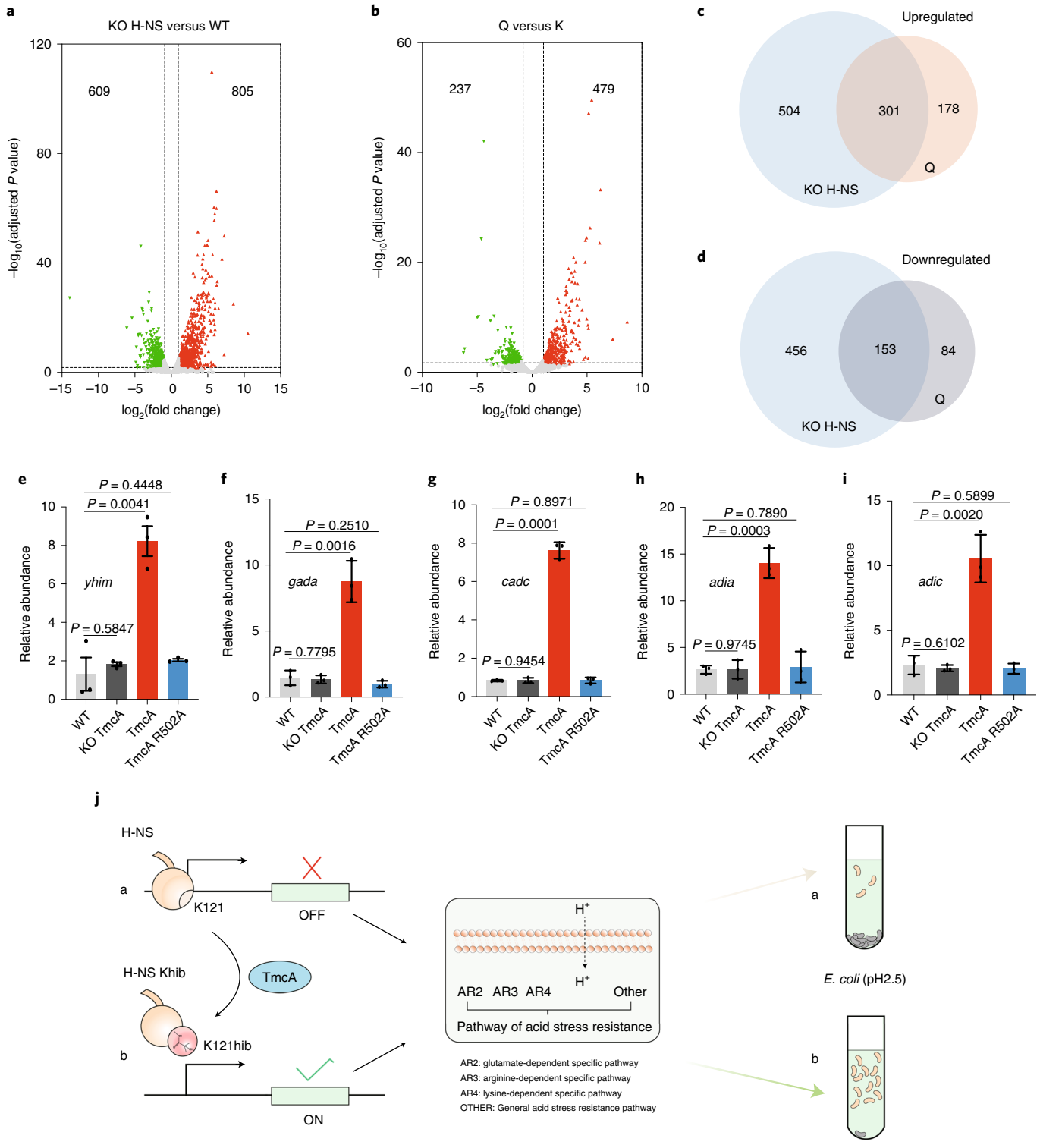

Fig. 6 | TmcA regulates K121hib of H-NS to promote the transcription of acid-resistance-related genes under acid stress. a,**b**, Volcano plots showing differentially expressed genes in various *E. coli* MG1655 strains: WT versus H-NS KO strain (**a**), H-NS KO strain harboring H-NS K121Q (Q) versus H-NS KO strain harboring H-NS (K) (**b**). False-discovery rate analysis of variance < 0.01, $n = 3$ biological repetitions. **c**,**d**, Venn diagrams showing comparison of differentially expressed genes among different strains. Upregulated genes of WT versus H-NS KO strain compared with upregulated genes of Q versus K (**c**); downregulated genes of WT versus H-NS KO strain compared with downregulated genes of Q versus K (**d**). **e**–**i**, Use of RT-qPCR to detect mRNA levels of acid-resistance-related genes (*yhia* (**e**), *gada* (**f**), *cadc* (**g**), *adia* (**h**), *adic* (**i**) in WT, TmcA KO, overexpressing TmcA and overexpressing TmcA R502A (data presented as mean ± s.e.m., two-tailed *t*-test, $n = 3$ biological repetitions). **j**, Schematic diagram of the mechanism of regulation by TmcA of H-NS K121hib involved in acid resistance.

influenced DNA binding of H-NS, so we reasonably hypothesized that H-NS K121hib may have an effect on bacterial acid tolerance. We thus performed a growth assay under extreme acid stress (1 h of incubation in lysogeny broth (LB) medium acidified to pH 2.5 by HCl). The stimulated cells were diluted in tenfold steps and cultured on LB plates. As shown in Fig. 5c, survival of the H-NS KO strain was obviously increased compared to WT *E. coli* MG1655, a result consistent with a previous report[34]. Next, we performed assays with complemented strains including WT H-NS, K121Q H-NS and K121R H-NS, finding a low survival rate of complementing WT H-NS and K121R H-NS, but highly improved survival in K121Q H-NS (similar to that in the H-NS KO strain), suggesting that H-NS K121hib can enhance the survival rate of *E. coli* under extreme acidic conditions (Fig. 5d,e). Performing assays in KO TmcA, overexpressing TmcA and overexpressing R502A TmcA *E. coli* strains (R502A TmcA), we further found that survival was significantly increased in the overexpressing TmcA strain (TmcA), where the K121hib level of H-NS was increased, but survival could not be ensured in the KO TmcA or overexpressing R502A TmcA strains (no change in K121hib level) under extreme acid stress (Fig. 5d,f). These findings show that bacterial acid tolerance is associated with the K121hib level of H-NS. Together, these results indicate that TmcA mediates H-NS K121hib to enhance the survival of *E. coli* under extreme acidic conditions.

TmcA-mediated H-NS K121hib regulation of transcription. To further investigate the mechanism of H-NS K121hib in enhancement of acid resistance, we performed RNA-seq in five strains containing WT, KO H-NS and complemented strains (H-NS, K121Q H-NS and K121R H-NS) cultured in LB medium (pH 2.5) for 1 h. Consistent with previous findings[34], gene expression profiles of KO H-NS *E. coli* were obviously distinguished from the WT strain: 609 genes were downregulated and 805 were upregulated in KO H-NS *E. coli* compared to the WT strain (Fig. 6a). Interestingly, and similar to KO H-NS *E. coli*, we found that K121Q H-NS also differed significantly from the H-NS strain: 237 genes were downregulated and 479 were upregulated in strain K121Q H-NS relative to H-NS (Fig. 6b). Venn diagrams produced showed the upregulated and downregulated genes of KO H-NS versus WT and K121Q H-NS versus H-NS, with >50% identical in the two strains (Fig. 6c,d), indicating that gene expression in K121Q H-NS is similar to that in KO H-NS. Meanwhile, there were essentially no obvious differences among WT, H-NS and K121R H-NS (Extended Data Fig. 7). One possible explanation is that K121hib causes H-NS to dissociate from DNA due to a reduction in electrostatic effect, and then promotes gene transcription. Furthermore, heatmap analysis of the five strains showed that genes related to acid tolerance were upregulated in KO H-NS and K121Q H-NS (Extended Data Fig. 8). It is clearly seen that the genes of glutamate-, arginine- and lysine-dependent acid tolerance systems were significantly upregulated in K121Q H-NS compared to H-NS strain (Supplementary Table 6 and Extended Data Fig. 9a) while they were unchanged in K121R H-NS and H-NS (Extended Data Fig. 8). These results imply that K121hib of H-NS promotes the transcription of genes related to acid tolerance. To further validate messenger RNA levels of acid tolerance genes (listed in Supplementary Table 6), we performed RT–qPCR assays for nine key genes (*yhim*, *gada*, *gadw*, *gadb*, *gadc*, *gade*, *adic*, *adia* and *cadc*). Consistent with RNA-seq assay, expression of these genes was also markedly upregulated in the overexpressing TmcA strain compared to WT, KO TmcA and the overexpressing R502A TmcA strain (Fig. 6e–i and Extended Data Fig. 9b–e). This provides further confirmation that K121hib causes H-NS to dissociate from DNA, promoting the transcription of genes related to acid tolerance, and thus bacterial survival is improved in overexpressing TmcA or K121Q H-NS strains (significantly increased K121hib of H-NS). Finally, it was concluded that TmcA mediates Khib of H-NS to regulate transcription for improvement in bacterial acid resistance (Fig. 6j).

Discussion

The NAPs function like histones, playing important roles in modulation of DNA structure and transcription in prokaryotes[36,37]. Emerging evidence indicates that PTMs on NAPs may be critical for the regulation of transcription in bacteria—for example, lysine acetylation on HBsu modulated nucleoid compaction in *Bacillus subtilis*[15] and lysine methylation on HupB regulated phenotypic resistance to isoniazid in mycobacteria[14]. However, understanding of the functions of PTMs on NAPs to date remains limited. Recently, we found a number of Khib localized on NAPs in *E. coli*[21], suggesting a potential effect of Khib on regulation of NAP functions in prokaryotes.

Insights into PTM functions are usually sparked by the identification of catalytic enzymes capable of adding PTM to substrates. It is believed that the generation of nearly all lysine acylation requires the formation of amide bonds, which can be catalyzed by binding of acetyltransferases with different acyl-CoA in eukaryotes[38]—for example, P300 was reported to catalyze diverse lysine modifications such as acetylation and crotonylation[22,39]. We reasonably speculated therefore that it is likely that KATs may also have activity toward Khib in *E. coli*. Given that GNAT is the only known acetyltransferase in *E. coli*[17,24,25], we constructed 18 GNATs overexpressing *E. coli* BL21 (DE3) strains and thereby screened out TmcA as a 2-hydroxyisobutyryltransferase and confirmed its enzymatic activity both in vitro and intracellularly. TmcA has been identified as an ATP-dependent RNA acetyltransferase[26,27], and here we demonstrate that TmcA is a lysine 2-hydroxyisobutyryltransferase while R502 is an essential site for the Khib enzymatic activity of TmcA and has no obvious lysine acetyltransferase activity. Notably, NAT10 acts as both a RNA cytidine acetyltransferase and a protein lysine acetyltransferase[40,41] in eukaryotes; however, it is extremely rare that an acyltransferase catalyzes modification on both RNA and proteins. Thus, our findings expand exploration of the functional diversity of acyltransferase catalysis.

To better understand the diverse functions of PTMs, it is necessary to establish an enzyme substrate regulatory network. Remarkably, 467 endogenous Khib candidate sites significantly regulated by TmcA were identified in *E. coli* using a quantitative proteomics approach. Pathways enrichment analysis showed that these candidates are associated with many prokaryotic cellular processes, especially in transcription and translation, suggesting the preference of TmcA as a lysine 2-hyroxyisobutyryltransferase. Therefore, our findings reveal systems attributes of TmcA targets and provide a resource dataset for understanding the function of TmcA-mediated Khib in diverse biological processes in prokaryotes.

Remarkably, a number of Khib sites were identified on NAPs (containing H-NS, HupA and HupB) of *E. coli* in this study, suggesting that Khib might have effects on NAP functions. Interestingly, only K121hib of H-NS was significantly decreased in the strain TmcA KO compared with WT and our study further demonstrated that TmcA can specifically regulate K121hib of H-NS both intracellularly and in vitro. It is well known that H-NS is a universal negative regulator for a dynamic genome that binds extensively to AT-rich DNA regions for inhibition of transcription[13,28,29], and influences bacterial chromatin organization[36,42]. Moreover, H-NS can regulate gene transcription to influence stress response (acid, base and high-salt stresses)[34,35,43]. However, it remains unclear whether PTM on H-NS is involved in the regulation of transcription and therefore it is appropriate to investigate the effect of K121hib on the function of H-NS. EMSA assays demonstrated that K121hib decreased the DNA-binding ability of H-NS. Furthermore, we found that upregulation of H-NS K121hib by TmcA can increase the survival rate of *E. coli* under extreme acid stress. RNA-seq data illustrated that H-NS K121hib induced an increase in acid-resistant

gene transcription, and RT–qPCR analysis further confirmed that a TmcA-overexpressing strain promoted transcription. Together, these data demonstrate that TmcA upregulates H-NS K121hib to decrease the DNA-binding ability of H-NS, promotes acid-resistant gene transcription and finally increases the survival of *E. coli* under acid stress. Thus we have dissected an important molecular mechanism of TmcA-mediated Khib in the regulation of transcription, and demonstrate a new PTM-mediated regulatory model of acid resistance in bacteria. Notably, with bacteria as an important source of fermentation products, this discovery also provides a new insight into solving the inevitable problems caused by environmental acid pressure in industrial production.

In summary, we originally identified TmcA as a lysine 2-hydroxyisobutyryltransferase for transcription regulation in bacteria, and showed that R502 is a key site for TmcA in regard to its 2-hydroxyisobutyryltransfer activity. Consequently we profiled endogenous candidates of TmcA containing 467 Khib sites, providing a framework to investigate the diverse functions of Khib regulated by TmcA in prokaryotes. Importantly, our results show that TmcA can regulate the DNA-binding ability of H-NS by increasing K121hib, which further affects transcription and cell survival under acid stress. Our work offers a new insight into the Khib-mediated regulation of transcription and acid resistance in bacteria.

Online content

Any methods, additional references, Nature Research reporting summaries, source data, extended data, supplementary information, acknowledgements, peer review information; details of author contributions and competing interests; and statements of data and code availability are available at https://doi.org/10.1038/s41589-021-00906-3.

Received: 15 March 2021; Accepted: 23 September 2021;
Published online: 13 December 2021

References

1. Park, J. et al. SIRT5-mediated lysine desuccinylation impacts diverse metabolic pathways. *Mol. Cell* **50**, 919–930 (2013).
2. Rardin, M. J. et al. SIRT5 regulates the mitochondrial lysine succinylome and metabolic networks. *Cell Metab.* **18**, 920–933 (2013).
3. Choudhary, C., Weinert, B. T., Nishida, Y., Verdin, E. & Mann, M. The growing landscape of lysine acetylation links metabolism and cell signalling. *Nat. Rev. Mol. Cell Biol.* **15**, 536–550 (2014).
4. Zhao, S. et al. Regulation of cellular metabolism by protein lysine acetylation. *Science* **327**, 1000–1004 (2010).
5. Harmel, R. & Fiedler, D. Features and regulation of non-enzymatic post-translational modifications. *Nat. Chem. Biol.* **14**, 244–252 (2018).
6. Sreelatha, A. et al. Protein AMPylation by an evolutionarily conserved pseudokinase. *Cell* **175**, 809–821 (2018).
7. Chambers, K. A. & Scheck, R. A. Bacterial virulence mediated by orthogonal post-translational modification. *Nat. Chem. Biol.* **16**, 1043–1051 (2020).
8. Sabari, B. R., Zhang, D., Allis, C. D. & Zhao, Y. Metabolic regulation of gene expression through histone acylations. *Nat. Rev. Mol. Cell Biol.* **18**, 90–101 (2017).
9. Wagner, E. J. & Carpenter, P. B. Understanding the language of Lys36 methylation at histone H3. *Nat. Rev. Mol. Cell Biol.* **13**, 115–126 (2012).
10. Zhang, D. et al. Metabolic regulation of gene expression by histone lactylation. *Nature* **574**, 575–580 (2019).
11. Semer, M. et al. DNA repair complex licenses acetylation of H2AZ1 by KAT2A during transcription. *Nat. Chem. Biol.* **15**, 992–1000 (2019).
12. Browning, D. F., Grainger, D. C. & Busby, S. J. Effects of nucleoid-associated proteins on bacterial chromosome structure and gene expression. *Curr. Opin. Microbiol.* **13**, 773–780 (2010).
13. Dillon, S. C. & Dorman, C. J. Bacterial nucleoid-associated proteins, nucleoid structure and gene expression. *Nat. Rev. Microbiol.* **8**, 185–195 (2010).
14. Sakatos, A. et al. Posttranslational modification of a histone-like protein regulates phenotypic resistance to isoniazid in mycobacteria. *Sci. Adv.* **4**, eaao1478 (2018).
15. Carabetta, V. J., Greco, T. M., Cristea, I. M. & Dubnau, D. YfmK is an N(ε)-lysine acetyltransferase that directly acetylates the histone-like protein HBsu in *Bacillus subtilis*. *Proc. Natl Acad. Sci. USA* **116**, 3752–3757 (2019).
16. Dai, L. et al. Lysine 2-hydroxyisobutyrylation is a widely distributed active histone mark. *Nat. Chem. Biol.* **10**, 365–370 (2014).
17. Huang, H. et al. p300-Mediated lysine 2-hydroxyisobutyrylation regulates glycolysis. *Mol. Cell* **70**, 663–678 (2018).
18. Huang, H. et al. Landscape of the regulatory elements for lysine 2-hydroxyisobutyrylation pathway. *Cell Res.* **28**, 111–125 (2018).
19. Huang, J. et al. 2-Hydroxyisobutyrylation on histone H4K8 is regulated by glucose homeostasis in *Saccharomyces cerevisiae*. *Proc. Natl Acad. Sci. USA* **114**, 8782–8787 (2017).
20. Dong, H. et al. Systematic identification of lysine 2-hydroxyisobutyrylated proteins in *Proteus mirabilis*. *Mol. Cell. Proteomics* **17**, 482–494 (2018).
21. Dong, H. et al. Protein lysine de-2-hydroxyisobutyrylation by CobB in prokaryotes. *Sci. Adv.* **5**, eaaw6703 (2019).
22. Sabari, B. R. et al. Intracellular crotonyl-CoA stimulates transcription through p300-catalyzed histone crotonylation. *Mol. Cell* **58**, 203–215 (2015).
23. Dancy, B. M. & Cole, P. A. Protein lysine acetylation by p300/CBP. *Chem. Rev.* **115**, 2419–2452 (2015).
24. Christensen, D. G. et al. Mechanisms, detection, and relevance of protein acetylation in prokaryotes. *mBio* **10**, e02708-18 (2019).
25. Christensen, D. G. et al. Identification of novel protein lysine acetyltransferases in *Escherichia coli*. *mBio* **9**, e01905-18 (2018).
26. Ikeuchi, Y., Kitahara, K. & Suzuki, T. The RNA acetyltransferase driven by ATP hydrolysis synthesizes N4-acetylcytidine of tRNA anticodon. *EMBO J.* **27**, 2194–2203 (2008).
27. Chimnaronk, S. et al. RNA helicase module in an acetyltransferase that modifies a specific tRNA anticodon. *EMBO J.* **28**, 1362–1373 (2009).
28. Dorman, C. J. H-NS: a universal regulator for a dynamic genome. *Nat. Rev. Microbiol.* **2**, 391–400 (2004).
29. Tendeng, C. & Bertin, P. N. H-NS in Gram-negative bacteria: a family of multifaceted proteins. *Trends Microbiol.* **11**, 511–518 (2003).
30. Weinert, B. T. et al. Lysine succinylation is a frequently occurring modification in prokaryotes and eukaryotes and extensively overlaps with acetylation. *Cell Rep.* **4**, 842–851 (2013).
31. Weinert, B. T. et al. Acetyl-phosphate is a critical determinant of lysine acetylation in *E. coli*. *Mol. Cell* **51**, 265–272 (2013).
32. Dilweg, I. W. & Dame, R. T. Post-translational modification of nucleoid-associated proteins: an extra layer of functional modulation in bacteria? *Biochem. Soc. Trans.* **46**, 1381–1392 (2018).
33. Hommais, F. et al. Large-scale monitoring of pleiotropic regulation of gene expression by the prokaryotic nucleoid-associated protein, H-NS. *Mol. Microbiol.* **40**, 20–36 (2001).
34. Gao, X. et al. Engineered global regulator H-NS improves the acid tolerance of *E. coli*. *Microb. Cell Fact.* **17**, 118 (2018).
35. Krin, E., Danchin, A. & Soutourina, O. Decrypting the H-NS-dependent regulatory cascade of acid stress resistance in *Escherichia coli*. *BMC Microbiol.* **10**, 273 (2010).
36. Wang, W., Li, G. W., Chen, C., Xie, X. S. & Zhuang, X. Chromosome organization by a nucleoid-associated protein in live bacteria. *Science* **333**, 1445–1449 (2011).
37. Dame, R. T., Rashid, F. Z. M. & Grainger, D. C. Chromosome organization in bacteria: mechanistic insights into genome structure and function. *Nat. Rev. Genet.* **21**, 227–242 (2020).
38. Zhao, S., Zhang, X. & Li, H. Beyond histone acetylation-writing and erasing histone acylations. *Curr. Opin. Struct. Biol.* **53**, 169–177 (2018).
39. Kaczmarska, Z. et al. Structure of p300 in complex with acyl-CoA variants. *Nat. Chem. Biol.* **13**, 21–29 (2017).
40. Liu, X. et al. NAT10 regulates p53 activation through acetylating p53 at K120 and ubiquitinating Mdm2. *EMBO Rep.* **17**, 349–366 (2016).
41. Ito, S. et al. Human NAT10 is an ATP-dependent RNA acetyltransferase responsible for N4-acetylcytidine formation in 18 S ribosomal RNA (rRNA). *J. Biol. Chem.* **289**, 35724–35730 (2014).
42. Dame, R. T., Noom, M. C. & Wuite, G. J. Bacterial chromatin organization by H-NS protein unravelled using dual DNA manipulation. *Nature* **444**, 387–390 (2006).
43. Krulwich, T. A., Sachs, G. & Padan, E. Molecular aspects of bacterial pH sensing and homeostasis. *Nat. Rev. Microbiol.* **9**, 330–343 (2011).

Methods

Construction of GNAT family genes overexpressing *E. coli* BL21 (DE3) strains. This method has been described previously[20,21]. In brief, plasmids of pET28a-GNATs, pET28a-hns, pBR322-hns-His tag and pBR322-TmcA-His tag were constructed to express GNAT family proteins and H-NS in *E. coli*. GNAT genes are listed in Supplementary Table 2. We cloned GNAT genes and hns gene selected Sph I and Sal I as restriction-enzyme-cutting sites to insert the genes into pET28a or pBR322. The constructed vectors of pET28a were transformed into *E. coli* BL21 (DE3) for overexpressing strains and cultured in LB medium containing kanamycin (Kana, 50 μg ml^{-1}), at 37 °C in shaken flasks to an optical density of 0.6–0.8 at 600 nm. Next, cells were induced with 0.05 mM IPTG at 37 °C for 4 h followed by harvesting of whole-cell lysates for immunoblotting or protein purification. The constructed vectors of pBR322-hns-His tag were transformed into H-NS KO *E. coli* MG1655, and the pBR322-TmcA-His tag vector was transformed into *E. coli* MG1655 and cultured in LB medium containing ampicillin (Amp, 50 μg ml^{-1}), at 37 °C in shaken flasks at 220 r.p.m. overnight. We used the Fast Mutagenesis System (TRANS) to construct the vectors containing point mutation genes. All primers used for PCR are listed in Supplementary Table 1.

Construction of KO *E. coli* MG1655 strains. The pCas vector was transformed into *E. coli* MG1655 and cultured in Kana LB plates at 30 °C, and the strain was induced through the Red recombination system of bacteriophage λ expression by arabinose. Guide RNA and the homologous arms of the target gene were constructed into the pTarget vector by PCR using the pEASY-Basic Seamless Cloning and Assmbly Kit (TRANS). The constructed pTarget vectors were transformed into *E. coli* containing pCas and cultured in Kana/Amp LB plates at 30 °C, and selected positive strains were cultured in LB medium with 0.5 mM IPTG at 30 °C for elimination of the constructed pTarget. Next, positive strains were cultured in LB medium at 37 °C for elimination of the pCas vector. All primers used for PCR are listed in Supplementary Table 1.

Simulation of binding of 2-hydroxyisobutyryl-CoA and TmcA. Autodock 1.5.6 was adopted to simulate the binding of 2-hydroxyisobutyryl-CoA and TmcA[44]. We employed the crystal structure of TmcA complexed with acetyl-CoA (PDB: 4R3U) and that of 2-hydroxyisobutyryl-CoA (PDB: 2zpa). Referring to the binding pocket of TmcA binding with acetyl-CoA, we placed 2-hydroxyisobutyryl-CoA into the binding pocket for structural modeling. The docking parameters were as follows: 100 Lamarckian genetic algorithm runs, and the maximum number of energy evaluations was 25 million. The simulation box was fixed at the center of the substrate and the box size was set at 100 × 60 × 60 Å in all dimensions. The conformation with the highest binding energy model was considered the enzyme-bound conformation, and the binding structure was shown by UCSF Chimera[45] and LigPlot+.

Chemical synthesis of 2-hydroxyisobutyryl-CoA. We prepared 2-hydroxyisobutyryl-CoA as described previously[17]. Briefly, 12.2 mmol of dicyclohexylcarbodiimide in 50 ml of dimethylformamide (DMF) was added to a 50-ml DMF mixture solution containing 10 mmol of 2-hydroxyisobutyric acid and 1 ml of thiophenol dropwise. With stirring for 180 min at 4 °C, the reaction was terminated by the addition of 40 ml of cold water. The solution was extracted by 100 ml of ether and washed three times with saturated sodium chloride. After drying of the ether extract by anhydrous sodium sulfate, purification of residue was performed by silica gel column chromatography (eluted by a 20:1 mixture of ethyl acetate and hexane) followed by silica thin-layer chromatography (eluted by a 1:4 mixture of ethyl acetate and hexane). To 16 mg of purified S-phenyl-2-hydroxy-2-methylpropanethioate dissolved in 500 μl of sodium bicarbonate (0.1 M) was added 1 ml of sodium bicarbonate buffer containing 10 mg of sodium salt of CoA at 0 °C. After resting overnight, the reaction was stopped by the addtion of 1 N HCl to pH 7.0. The final product was obtained by evaporation of water at 30 °C, followed by extraction with ether (8 ml five times) and ethyl acetate (8 ml eight times).

ITC measurement. This method was described previously[21]. Briefly, using the MicroCal PEAQ-ITC titration calorimeter (Malvern Instruments) at 37 °C, the reaction cell containing 50 μM proteins was titrated with 500 μM acetyl-CoA. The volume of the first injection was 0.5 μl of 500 μM acetyl-CoA, and the following 18 injections were 2.0 μl. The binding isotherm was fit with the Origin 7.0 software package (OriginLab). Each group had three biological repetitions.

LC–MS/MS analysis for ac4C. Total RNA for each sample (1 μg) was digested by nuclease P1 then incubated with alkaline phosphatase at 37 °C for 2 h; samples were dried, dissolved in 0.01% formic acid (buffer A) and injected for LC–MS/MS. Nucleosides were separated using a Waters ACQUITY UPLCTM HSS T3 column (2.1 × 100 mm^2, 1.7 μm) at a flow rate of 0.2 ml min^{-1} (column temperature, 25 °C) and analyzed using an Agilent 6600 QQQ triple-quadrupole mass spectrometer in positive electrospray ionization mode. A 40-min gradient was developed to obtain optimum separation of modified nucleosides (mobile phases included buffer A and 80% methanol in aqueous 0.01% formic acid as buffer B). Nucleosides were quantified by nucleoside-to-base ion mass transitions.

In vitro ac4C formation. The method used was previously described[26]. Briefly, we transcribed $tRNA^{Met}$ in vitro as substrate and 200 pmol of $tRNA^{Met}$ was incubated with 10 μl of reaction mixture (10 mM KCl, 10 mM $MgCl_2$, 10 mM DTT, 1 mM ATP, 1 mM acetyl-CoA, 100 mM Tris-HCl (pH 7.8) and 2 μg of recombinant TmcA). The tRNA was then digested into nucleosides with alkaline phosphatase and nuclease P1, and the final sample was dried and prepared for LC–MS/MS analysis.

SILAC labeling and sample preparation. As described previously[21], WT *E. coli* MG1655 and TmcA KO *E. coli* were cultured in M9 minimal medium with 0.2% glucose and L-lysine (100 mg ml^{-1}) (WT) or $^{13}C_6$-lysine (TmcA KO). Cells were then harvested during the mid-exponential phase of growth and lysate, washed three times with cold PBS and sonicated on ice in PBS. After centrifugation (20,000*g*) at 4 °C for 20 min, the supernatant was collected. Equal amounts of proteins from WT and TmcA KO were mixed and precipitated by trichloroacetic acid and precipitated proteins were dissolved in 100 mM NH_4HCO_3 with overnight digestion by trypsin (trypsin:protein ratio, 1:50), followed by a second digestion at a ratio of 1:100 for 4 h. Tryptic digestion was reduced with 10 mM DTT for 1 h at 37 °C, followed by alkylation with 20 mM iodoacetamide for 45 min at room temperature under darkness. Excess iodoacetamide was finally blocked with 20 mM cysteine.

Peptide fractionation and immunoaffinity enrichment. Tryptic peptides were separated and fractionated using high-pH, reversed-phase HPLC (L-3000 HPLC System, Rigol) on a Thermo HYPERSIL GOLD C18 column (5-μm particles, 175 Å, 10 × 250 mm^2) with gradient elution. For Khib enrichment, tryptic peptides were separated at a flow rate of 1 ml min^{-1} and monitored at 214 nm. The column oven was set at 40 °C. Eluent was collected every 1 min, with each component marked by time of collection and combined into 12 fractions. Each peptide fraction was redissolved in NETN buffer (50 mM Tris-HCl pH 8.0, 100 mM NaCl, 1 mM EDTA, 0.5% Nonidet P-40) and incubated with anti-2-hydroxyisobutyryllysine antibody-conjugated protein A agarose beads (PTM Biolabs) at 4 °C overnight, with gentle rotation. For Kac enrichment, tryptic peptides were redissolved in NETN buffer and incubated with anti-acetyl-lysine antibody-conjugated protein A agarose beads (PTM Biolabs) at 4 °C overnight, with gentle rotation. The beads were washed three times with NETN buffer, twice with ETN buffer (50 mM Tris-Cl pH 8.0, 100 mM NaCl and 1 mM EDTA) and three times with water. Bound peptides were eluted three times with 1% trifluoroacetic acid. Finally, the eluates were combined and dried and cleaned with C18 ZipTips (Millipore Corp) before nano-HPLC–MS/MS analysis.

HPLC–MS/MS analysis. Modified peptides were analyzed by HPLC–MS/MS as described previously[21]. Briefly, each sample of enriched Khib or Kac peptides was reconstituted in 0.1% formic acid and then injected into a nano-LC system (EASY-nLC 1000, Thermo Fisher Scientific). Peptides were resolved in a C18 column (50-μm inner diameter × 15 cm, 2-μm C18). Gradient elution was performed with 2–35% HPLC buffer B (0.1% formic acid in acetonitrile) for 110 min and 90% buffer B for 15 min, and the elutes were then subjected to electrospray ionization at 2.4 kV and transferred into an Orbitrap Q-Exactive Plus mass spectrometer (Thermo Fisher Scientific). Mass spectrometric analysis was carried out in data-dependent mode, cycling between acquisition of one MS (full MS scan range 350–1,800 *m/z* at 70,000 resolution) followed by MS/MS of the 15 most intense peaks (higher-energy collision dissociation (HCD) with normalized energy of 27%), and data were collected by Xcalibur (v.4.0.27.19).

Database search and data filtering criteria. The database search and filtering criteria were performed according to reported research[21]. Briefly, the acquired MS/MS spectra were searched against the UniProt *E. coli* MG1655 protein database using the MaxQuant engine (v.1.5.5.1). The overall false-discovery rate for peptides was set to <1%. The main search parameters were as follows: trypsin as the proteolytic enzyme; two permitted missed cleavages; seven amino acid residues as minimal peptide length; carbamidomethylation on Cys as fixed modification; oxidation of methionine, acetylation on the peptide N terminus and Khib as variable modifications; and mass error of ±10 ppm for precursor ions and ±0.02 Da for fragment ions. To improve the accuracy of 2-hydroxyisobutyrylated peptide identification, we further excluded peptides with a score of <40 or localization probability of <0.75. The ratios of quantified Khib peptides were further normalized by those of corresponding protein levels. The method used for Kac database search is the same as for Khib, except for switching from Khib to Kac as the variable modification.

In vitro Khib and acetylation assay. Purified recombinant TmcA (or mutant) and H-NS (or mutant) were incubated in a reaction buffer (100 mM Tris-HCl, 10 mM KCl, 10 mM $MgCl_2$ pH 7.8), or the purified recombinant YiaC and H-NS (or mutant) were incubated in a reaction buffer (50 mM HEPES-NaOH pH 7.5) with or without 1 mM ATP and in the presence or absence of 500 μM 2-hydroxyisobutyryl-CoA. The mixture was incubated at 37 °C for either 2 or 6 h, and the reaction products analyzed by SDS–polyacrylamide gel electrophoresis and immunoblotting with either pan-anti-Khib or pan-anti-Kac antibody (diluted 1:1000).

PRM analysis. PRM analysis was carried out on a Nano-LC coupled to an Orbitrap Q-Exactive Plus mass spectrometer. The method was performed as

described previously[21]. Briefly, peptides were resolved on a C18 column (50-μm inner diameter × 15 cm, 2-μm C18). The gradient elution was performed with 2–35% buffer B (0.1% formic acid in acetonitrile) for 110 min, and then with 90% buffer B for 15 min. The elute were subjected to electrospray ionization at 2.4 kV and transferred to a mass spectrometer. One full MS scan was followed by ten tandem MS scans in PRM mode (triggered by an inclusion list). For the full MS spectrum the parameters included a resolution of 70,000, 3×10^6 automatic gain control and 50 ms maximum injection time. For the MS/MS spectrum the parameters included a resolution of 17,500, 1×10^5 automatic gain control and 100 ms maximum injection time. The precursor ion was subjected to HCD with a normalized energy of 27%. Each sample was analyzed three times. The resulting PRM data were searched against the database-imported SILAC result using the Skyline daily engine. To verify the validity of identified Khib peptides and monitor the co-elution of synthetic and intracellular Khib peptides, the same PRM analyses were performed with synthetic peptides, cell lysate and mixtures. The ion chromatograms of Khib peptides were extracted from raw data.

EMSA assay. A 0.1 μM, 220-base pair DNA fragment of the *lac* promoter (a PCR fragment of the U19 plasmid cloned by primer: forward: CGGTAACCAGAACTCTCATAATTCGC, reverse: CGGCTAAATTCTTGTGTAAACGATTCC) was incubated at variable concentrations (0, 2, 4, 6, 8 μM) of H-NS (or mutants) in the binding buffer (50 mM NaCl and 20 mM Tris, pH 8.1). After equilibration for 10 min at 25 °C, loading dyes and glycerol (3 μl of buffer solution in 50% (v/v) glycerol) were added and the samples loaded on a 6% polyacrylamide gel at 80 V cm^{-1}. The gel was then visualized with ethydium bromide.

Acid shock assay. Strains were grown in LB medium (pH 7.0) at 37 °C overnight. Cultures were diluted to 1:100 in LB medium, grown to optical density 0.5 and cells were acidified with HCl to pH 2.5 and cultured for 1 h at 37 °C. After acidification for 1 h, cultures were serially diluted 1:10 with acidified LB medium (pH 2.5) in 96-well microplates. Before and after acid shock, cultures were plated on LB plates (pH 7.0) and incubated overnight at 37 °C.

RNA-seq. A TruSeq RNA Sample Prep Kit (Illumina) was used to prepare the RNA-seq libraries and to purify polyadenylated RNAs. Libraries were sequenced using HiSeq2500 (Illumina). After filtering using Bowtie2, filtered reads were mapped to reference transcripts. Next, gene expression levels were calculated by expectation maximization and differential expression genes were identified by DESeq2 algorithms based on gene expression levels[46]. |Fold change| ≥2 and adjusted $P < 0.05$ were selected as significantly differential expression genes. Each strain was analyzed with three biological replicates for statistical analysis.

RT–qPCR. After isolation from cells using the EasyPure RNA Kit (TRANS), total RNA was reverse transcribed using the cDNA Synthesis Kit (Thermo Scientific). Complementary DNAs were further analyzed using the StepOnePlus Real-Time PCR system (Applied Biosystems) with specific gene primers (listed in Supplementary Table 1). Meanwhile, 16S RNA levels were used as the standard curve to eliminate errors caused by dilution, and to quantify relative cDNA abundance. Melt-curve analysis was performed to ensure specific product amplification for each gene of primer pairs. Each sample had three biological repetitions and each biological sample had three repetitions. The data were analyzed using PRISM v.8.0.

Reporting Summary. Further information on research design is available in the Nature Research Reporting Summary linked to this article.

Data availability

All data required to evaluate the conclusions are present in the paper and in Supplementary information. The proteomics MS data have been deposited with the ProteomeXchange Consortium (http://proteomecentral.proteomexchange.org) via the iProX partner repository, with the dataset identifiers PXD024897 and PXD024901. RNA-seq data can be obtained at the Gene Expression Omnibus database under accession no. GSE169499. Source data are provided with this paper.

References

44. Morris, G. M. et al. AutoDock4 and AutoDockTools4: automated docking with selective receptor flexibility. *J. Comput. Chem.* **30**, 2785–2791 (2009).
45. Pettersen, E. F. et al. UCSF Chimera–a visualization system for exploratory research and analysis. *J. Comput. Chem.* **25**, 1605–1612 (2004).
46. Love, M. I., Huber, W. & Anders, S. Moderated estimation of fold change and dispersion for RNA-seq data with DESeq2. *Genome Biol.* **15**, 550 (2014).

Acknowledgements

This work was supported by funding from the National Natural Science Foundation of China to K.Z. (nos. 21874100 and 22074103), to H.D. (no. 32101023), to G.Z. (no. 21904097) and to X.B. (no. 22004091); and from the Talent Excellence Program from Tianjin Medical University, to K.Z.

Author contributions

K.Z. supervised experiments. H.D. and K.Z. designed experiments, analyzed the data and wrote the manuscript. H.D., J.Z. and Y.Z. carried out cell culture, enzymatic activity assay and molecular biological experiments. H.D., G.Z. and X.B. carried out proteomic survey. C.B. and H.D. carried out chemical synthesis. H.D., Y.H., S.T., D.H., L.X. and K.Z. carried out data collection, analysis and interpretation. All authors discussed the results and commented on the manuscript.

Competing interests

The authors declare no competing interests.

Additional information

Extended data is available for this paper at https://doi.org/10.1038/s41589-021-00906-3.

Supplementary information The online version contains supplementary material available at https://doi.org/10.1038/s41589-021-00906-3.

Correspondence and requests for materials should be addressed to Kai Zhang.

Peer review information *Nature Chemical Biology* thanks the anonymous reviewers for their contribution to the peer review of this work.

Reprints and permissions information is available at www.nature.com/reprints.

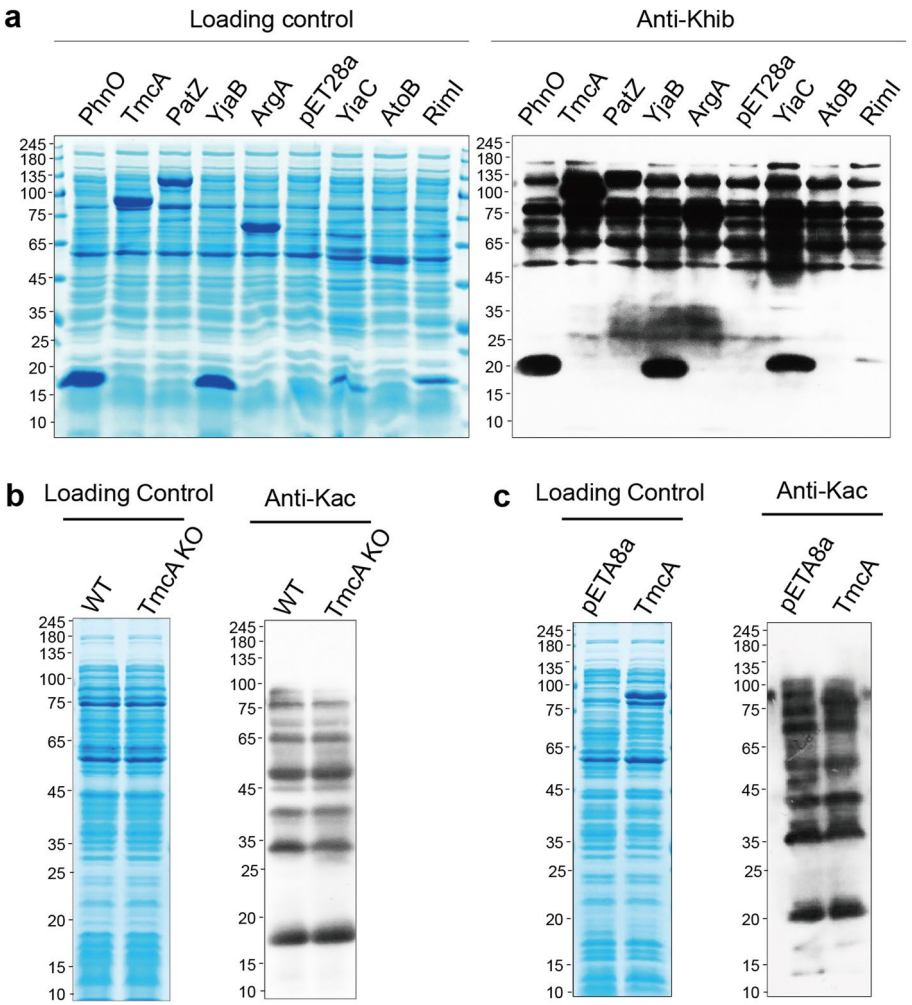

Extended Data Fig. 1 | Identification TmcA as potential lysine 2-hyroxyisobutyryltransferase, not a lysine acetyltransferase. a, Overexpression of TmcA and YiaC increase Khib in *E. coli*. *E. coli* BL21 were transferred with empty vector (pET28a) as control and GNAT-pET28a vectors for GNAT overexpressing strains, the Khib level of whole cell lysates were analyzed by western blotting. **b**, Overexpression of TmcA has no obvious effect on Kac in *E. coli*. *E. coli* BL21 were transferred with empty vector (pET28a) as control and TmcA-pET28a vector overexpressing strains, the Kac level of whole cell lysates were analyzed by western blotting. **c**, TmcA KO has no obvious effect on Kac in *E. coli*. Kac levels of TmcA KO *E. coli* MG1655 were analyzed by western blotting, WT as control. And each group had three biological repetitions. All western experiments had three biological repetitions with similar result.

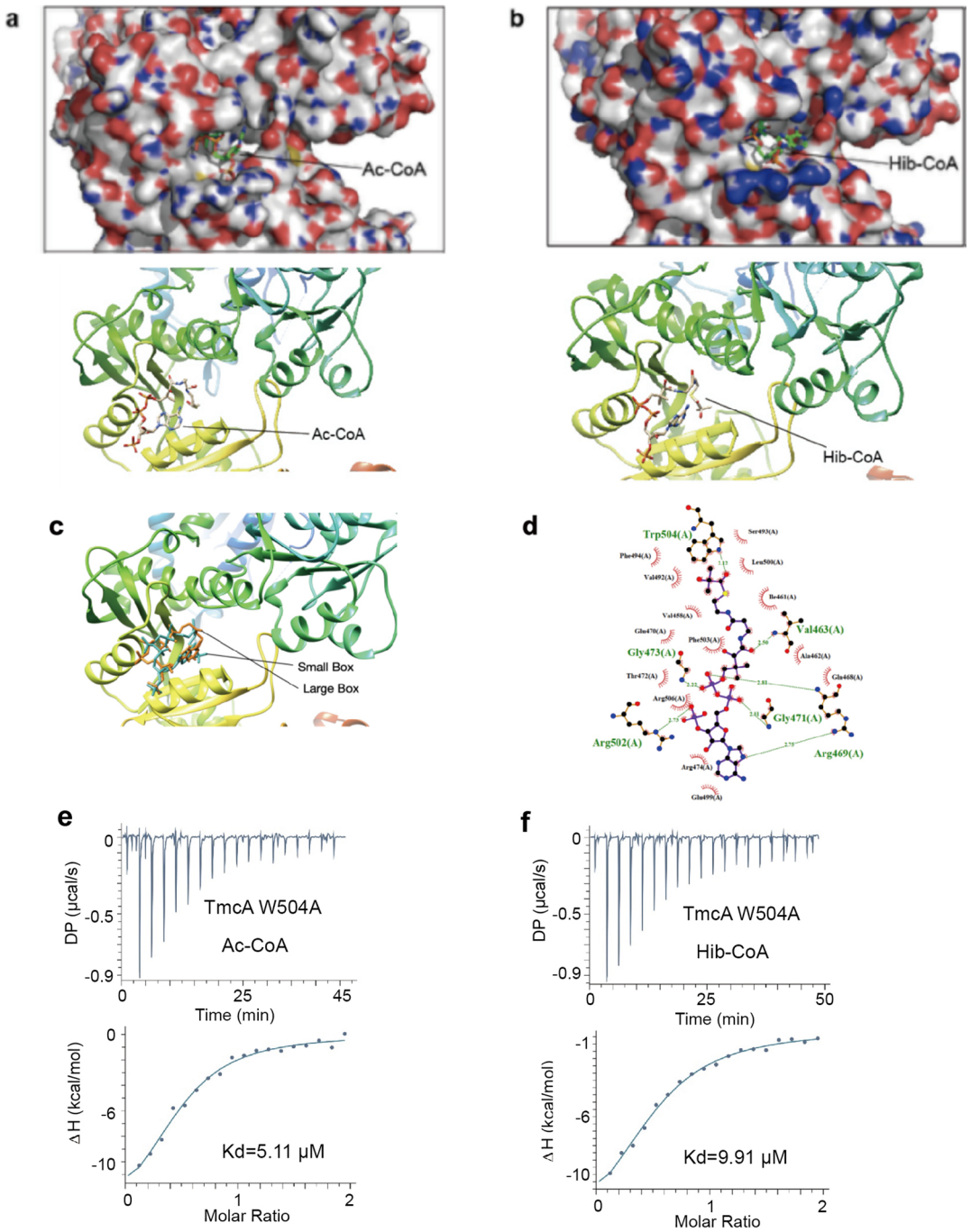

Extended Data Fig. 2 | TmcA can bind with 2-hydroxyisobutyryl-CoA. a, Structural modeling of TmcA combining acetyl-CoA. Exhibition the crystal structure of TmcA combining acetyl-CoA by UCSF Chimera. Ac-CoA: acetyl-CoA. Related to Fig. 2a. **b**, Structural modeling of TmcA combining 2-hydroxyisobutyryl-CoA. Using Autodock modes the binding of 2-hydroxyisobutyryl-CoA with TmcA and exhibits the crystal structure by UCSF Chimera. Hib-CoA: 2-hydroxyisobutyryl-CoA. **c**, Structural modeling of TmcA combining Hib-CoA under different setting of Box. Small box:100 Å × 60 Å × 60 Å, large box:120 Å × 80 Å × 80 Å. **d**, The hydrogen bonds and hydrophobic interaction between TmcA and Hib-CoA are shown by LigPlot+ with large box. **e-f**, ITC analysis of the affinity of recombinant W504A TmcA mutant with Ac-CoA and Hib-CoA separately, and each group had three biological repetitions, each group had three biological repetitions with similar result.

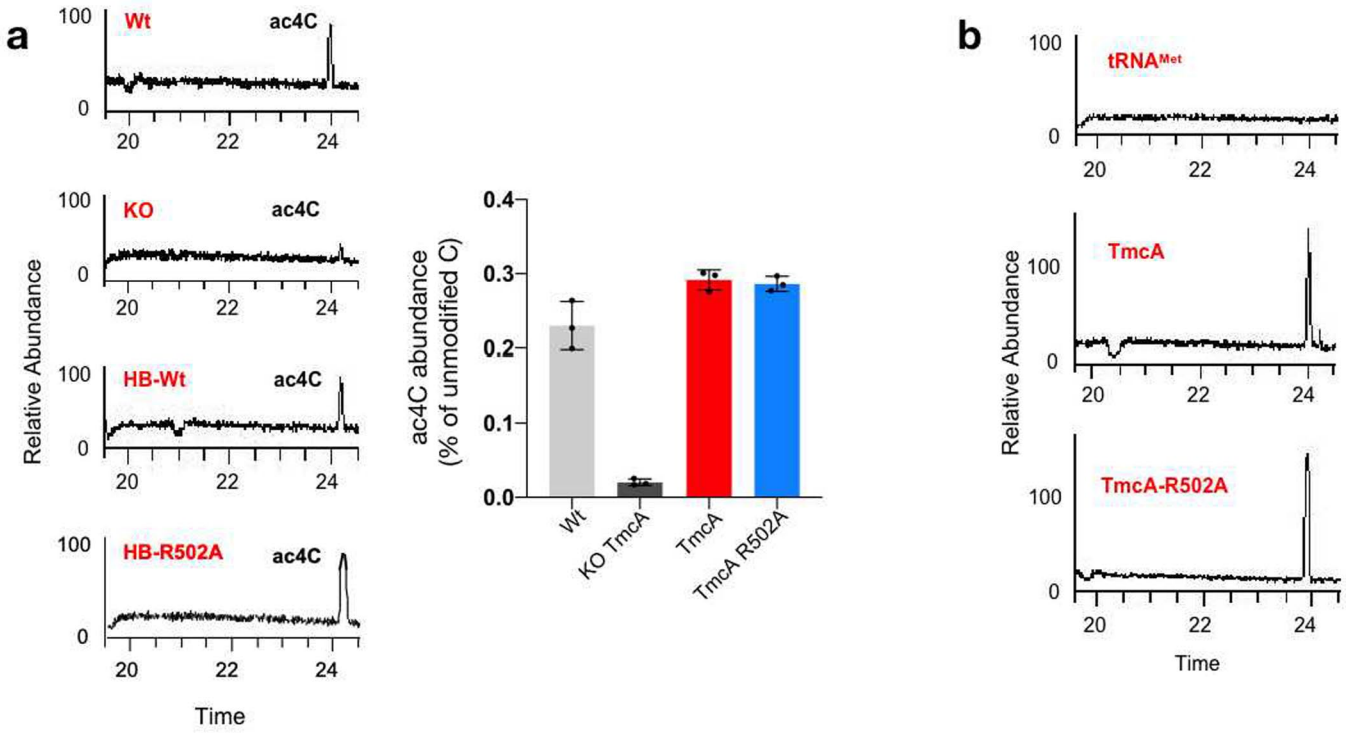

Extended Data Fig. 3 | LC-MS/MS detection ac4C intracellularly and *in vitro*. a, ac4C levels of wild type *E.coli* (WT), TmcA KO (KO), complementary TmcA (TmcA) and complementary TmcA R502 (TmcA R502) strains were detected by LC-MS/MS, each with three biological repetitions (data are presented as means ± SEM). **b**, The synthetic $tRNA^{Met}$ incubated with TmcA or TmcA R502 and detected the ac4C levels by LC-MS/MS. Each group had three biological repetitions with similar result.

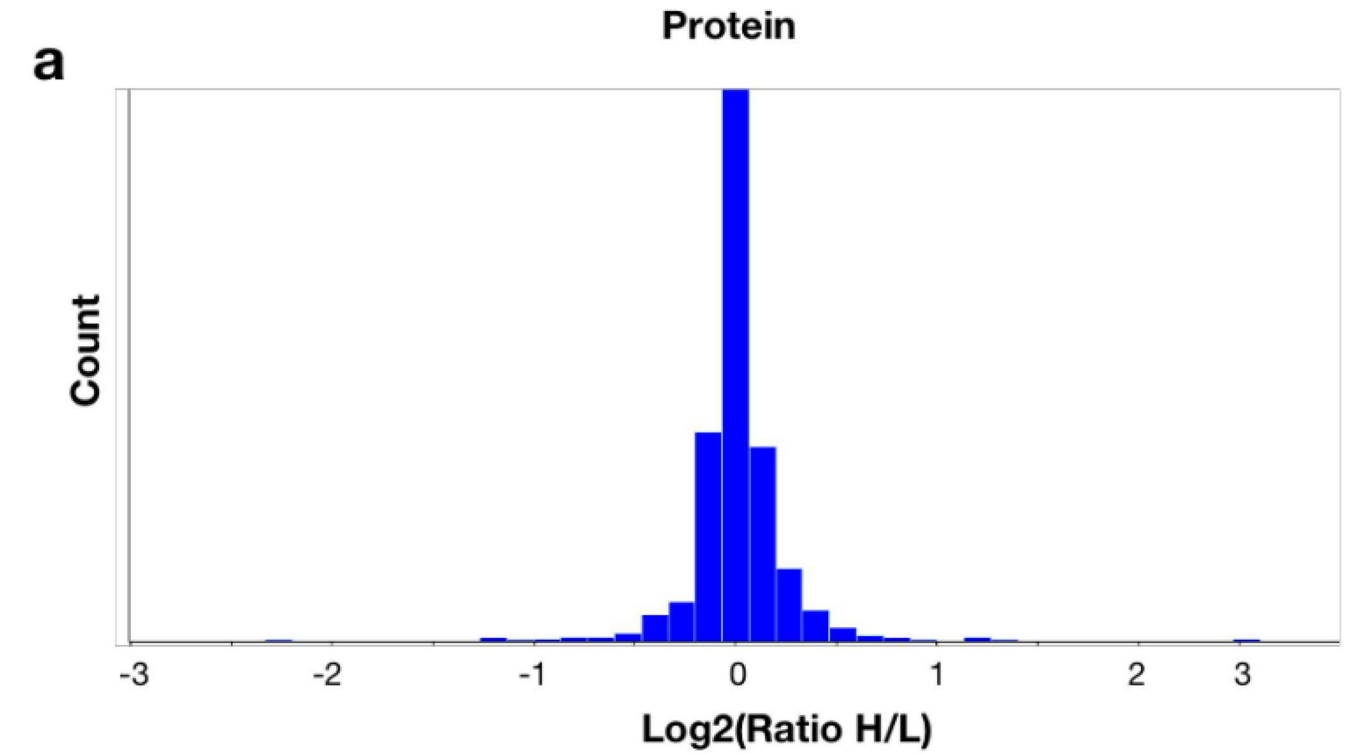

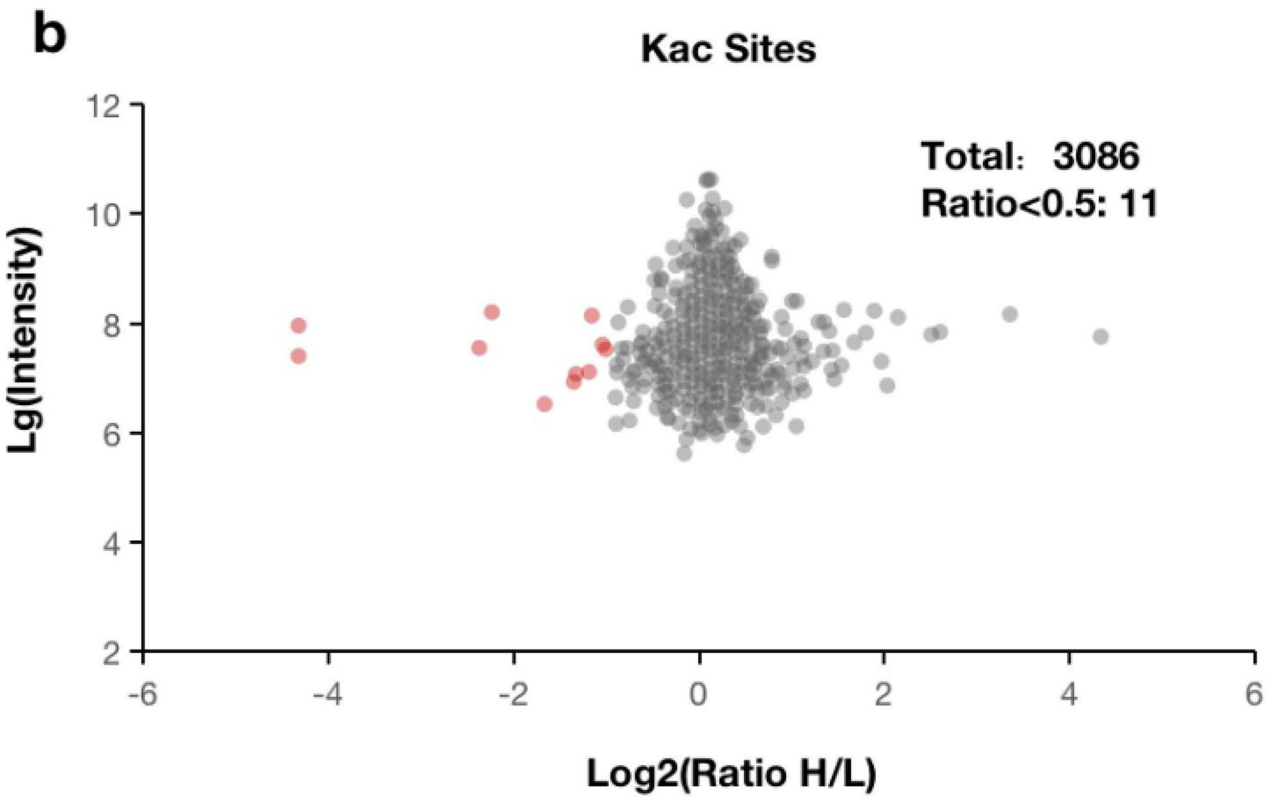

Extended Data Fig. 4 | Profiling the the endogenous substrate proteins for acetylation by TmcA in *E. coli*. a, Schematic representation of experimental workflow for the SILAC quantification of Khib in WT and TmcA KO *E. coli*. **b**, The histograms show experimentally determined relative protein abundance distributions for the samples used to analyze acetylation.

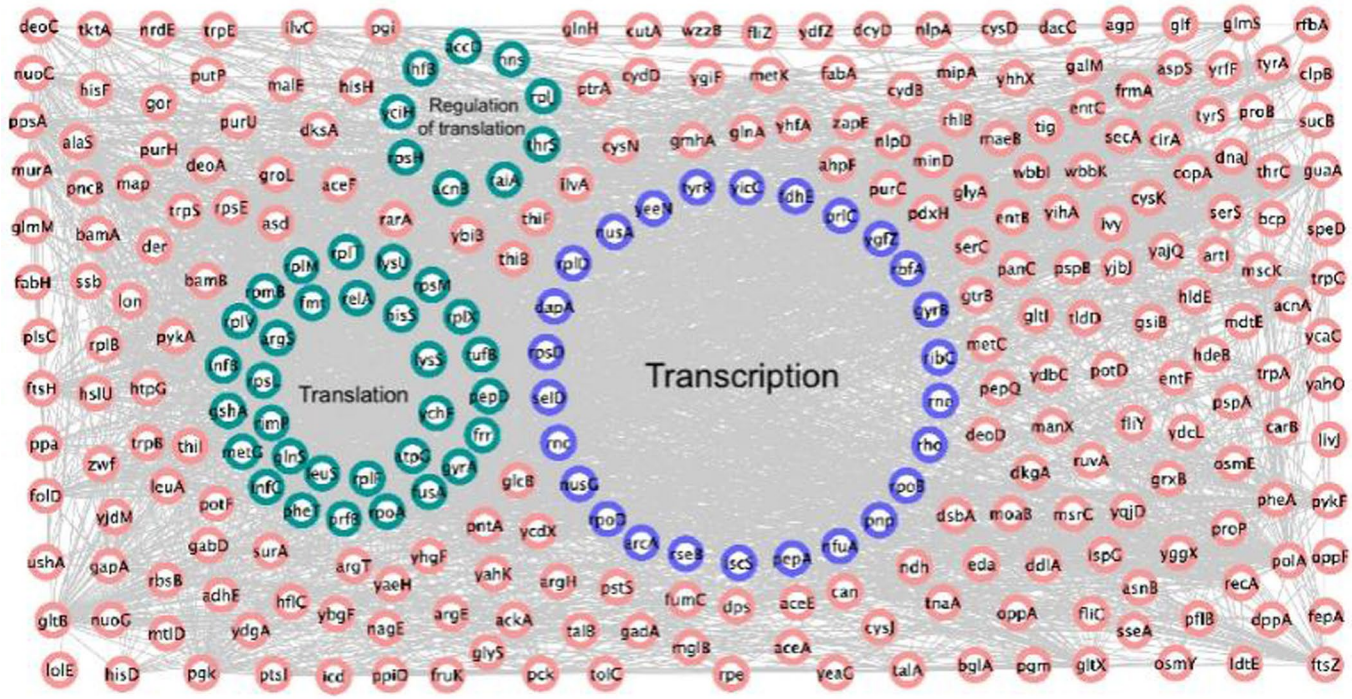

Extended Data Fig. 5 | TmcA-mediated Khib specifically related to transcription and translation. Shown is an interaction network of the TmcA-regulated Khib proteome based on the STRING database (v10). The network is visualized in Cytoscape 3.8.

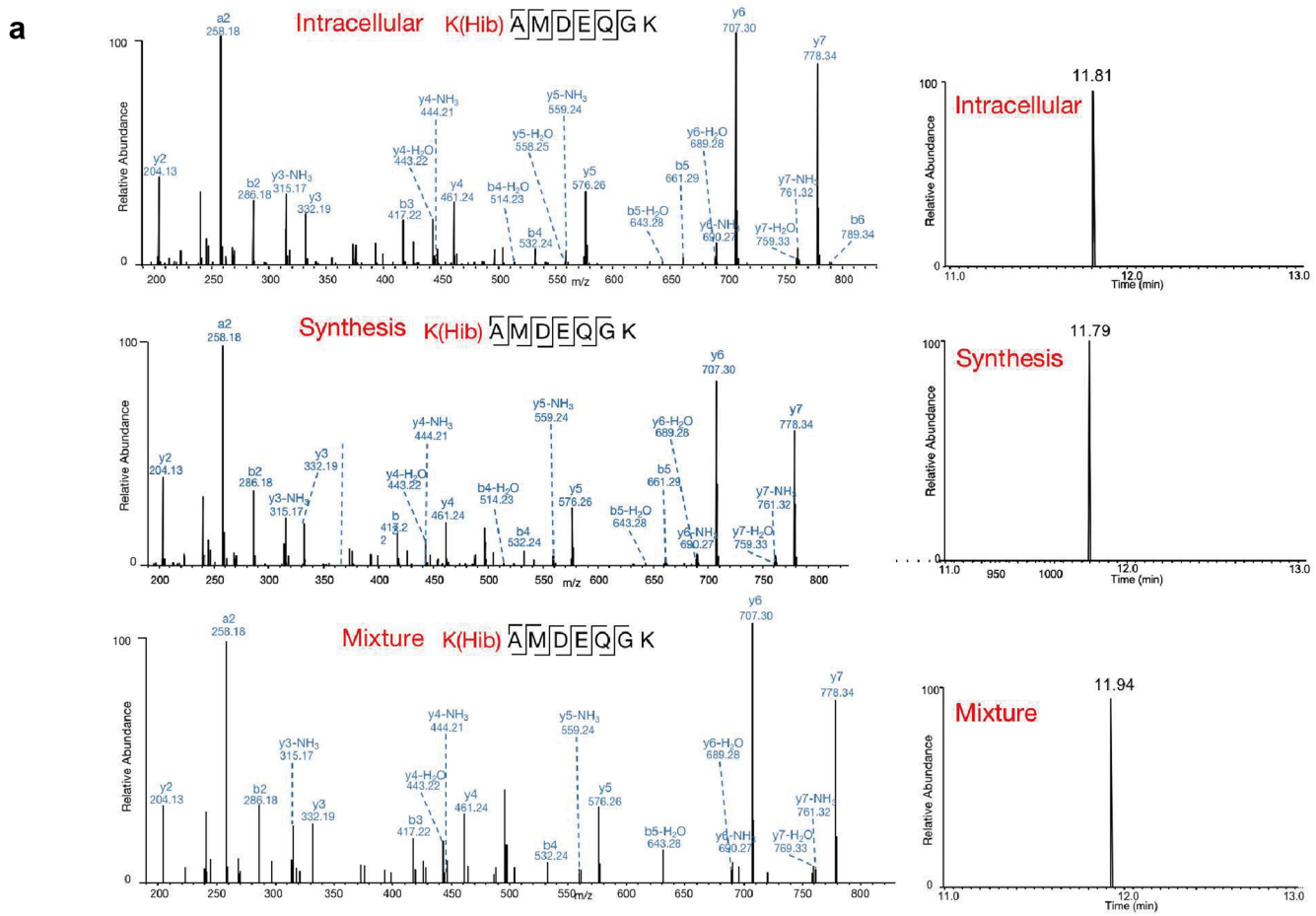

Extended Data Fig. 6 | The MS/MS spectrum of the intracellular tryptic peptide bearing Khib and its counterpart synthetic peptide. a, MS/MS spectrum of ASDVK(hib)DSSIR (sythesis, intracellular and both mixture) and the extracted ion chromatograms. **b**, Multiple protein sequences alignment of H-NS from different species.

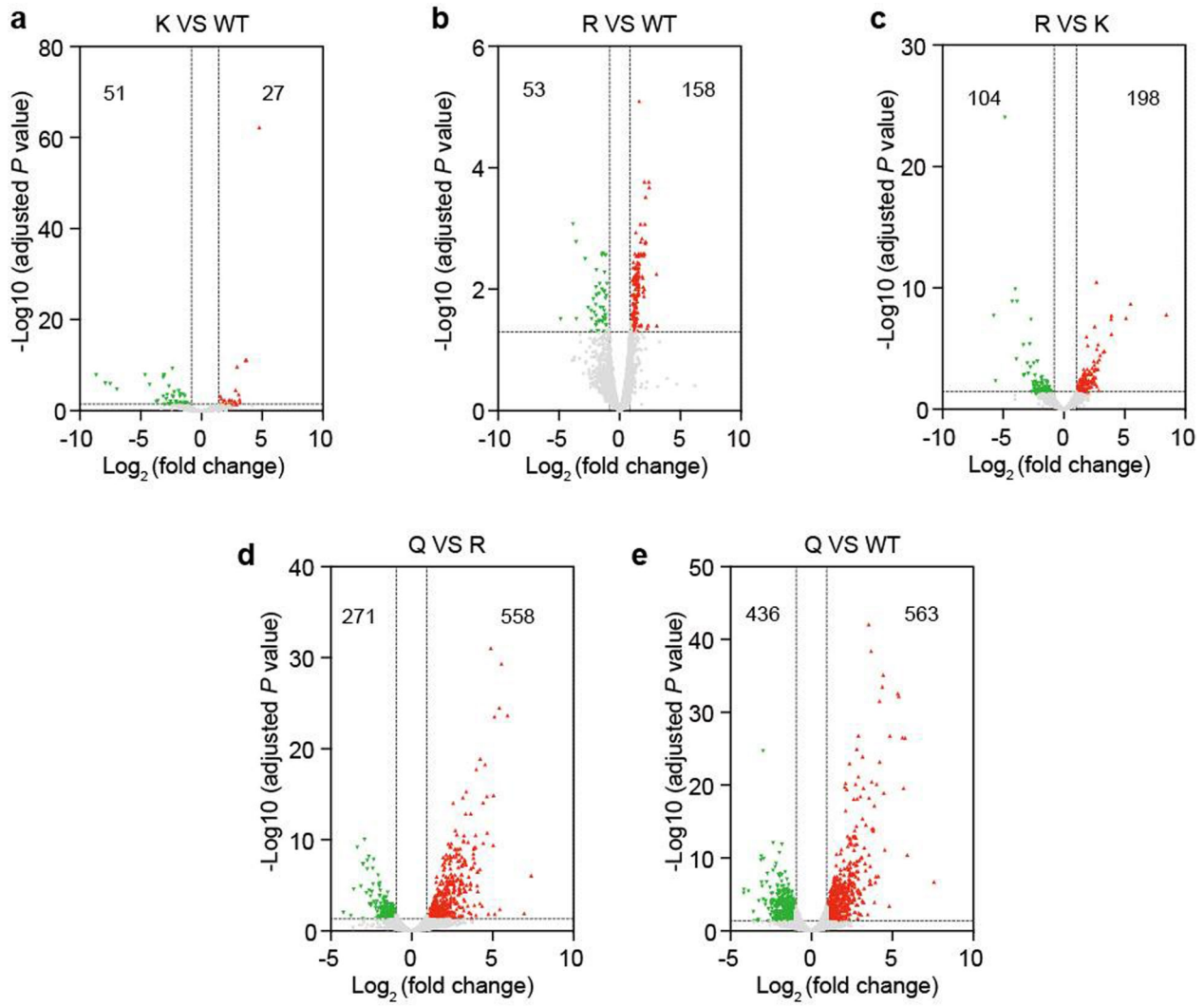

Extended Data Fig. 7 | Volcano plots showing differentially expressed genes in different *E. coli* MG1655 strains. WT: wild type *E. coli* MG1655, O: H-NS KO *E. coli* MG1655, K: H-NS KO strain harboring H-NS, Q: H-NS KO strain harboring H-NS K121Q, R: H-NS KO strain harboring H-NS K121R. FDR ANOVA < 0.01, n = 3 biological repetitions.

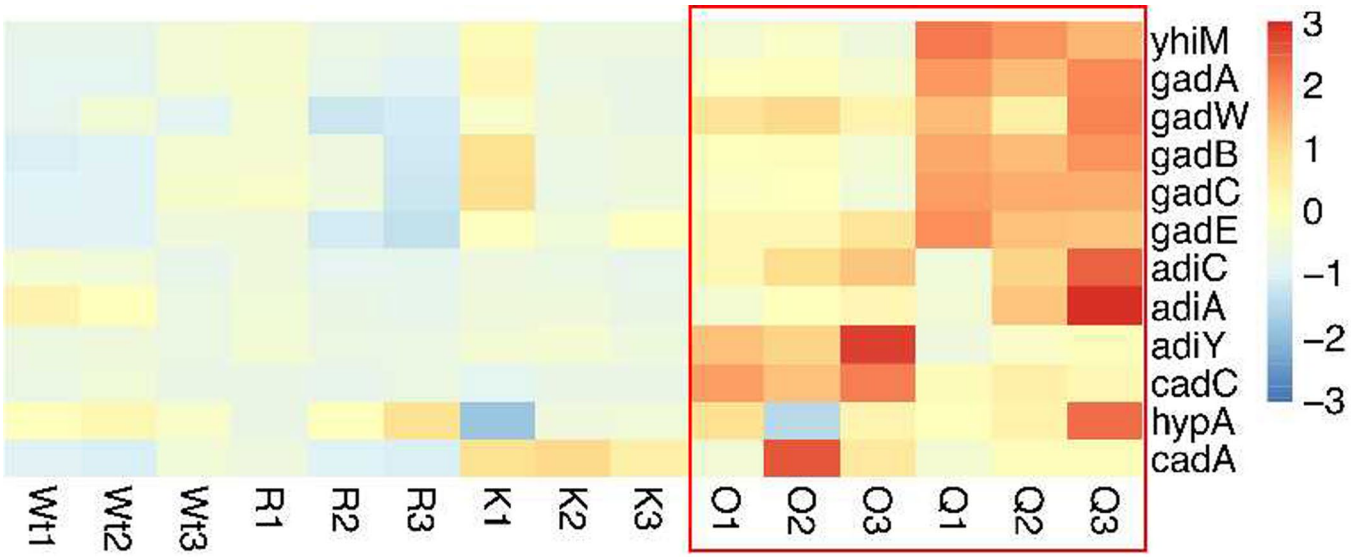

Extended Data Fig. 8 | Heatmap of acid resistance related gene expression values of different H-NS related strains. Rows show Z scores calculated for each group. Wt: wild type *E. coli* MG1655, O: H-NS KO *E. coli* MG1655, K: H-NS KO strain harboring H-NS, Q: H-NS KO strain harboring H-NS K121Q, R: H-NS KO strain harboring H-NS K121R.

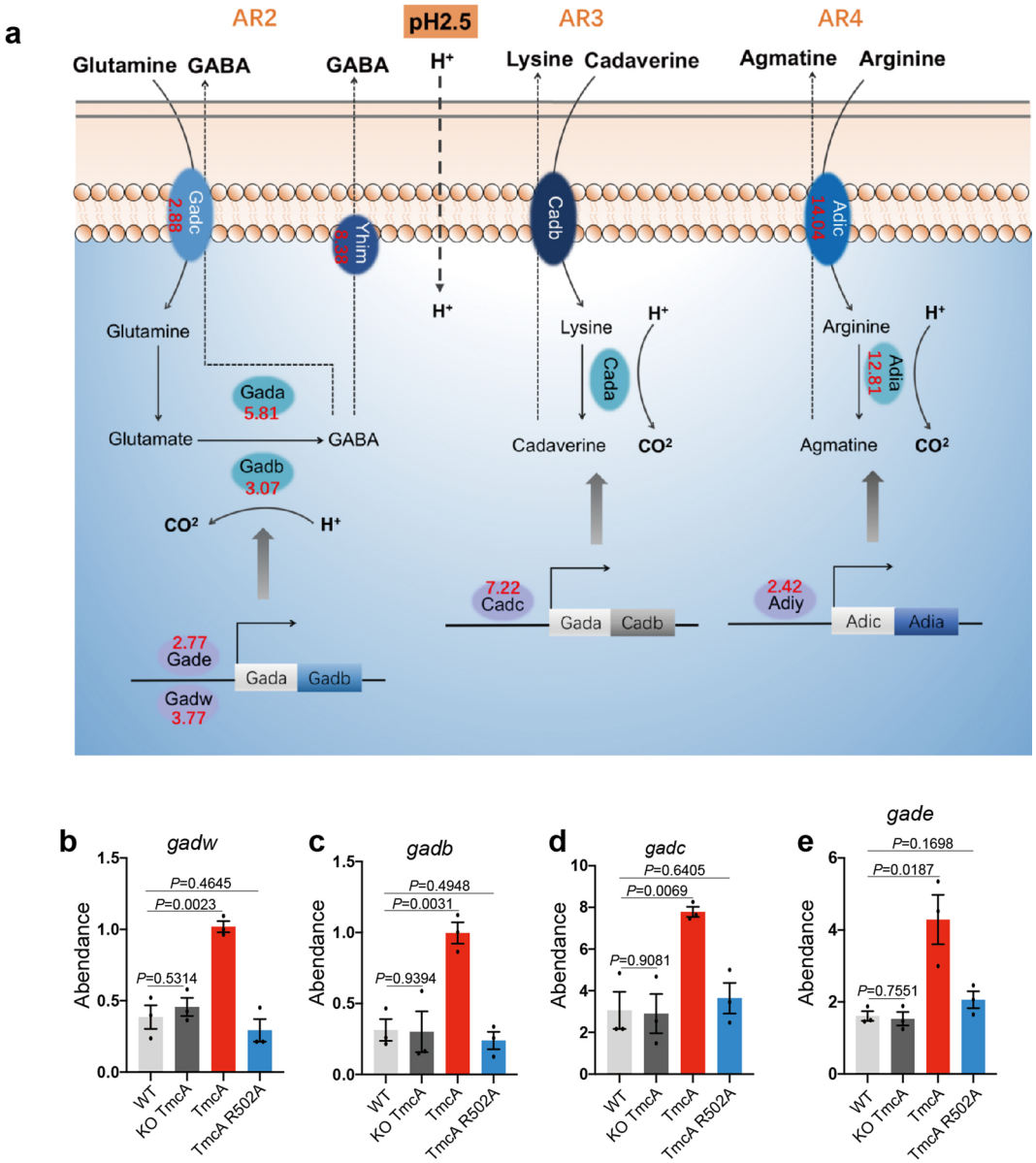

Extended Data Fig. 9 | Acid resistance related genes were increased in Q strain compared with K strain. a, AR2, AR3 and AR4 are the different mechanisms for acid resistance in *E. coli*, red numbers represent the difference multiple of gene expression compared Q versus K. The red numbers represent the multiple of gene up regulation. **b-e**, RT-qPCR detecting mRNA levels of acid resistance related genes in WT, TmcA KO strain, overexpressing TmcA strain and overexpressing TmcA R502A strain, and each group had three biological repetitions and each biological sample had three repetitions. (data are presented as means ± SEM, Two-tailed t-test, n = 3 biological repetitions).

nature research

Corresponding author(s): Kai Zhang

Last updated by author(s): Aug 24, 2021

Reporting Summary

Nature Research wishes to improve the reproducibility of the work that we publish. This form provides structure for consistency and transparency in reporting. For further information on Nature Research policies, see our Editorial Policies and the Editorial Policy Checklist.

Statistics

For all statistical analyses, confirm that the following items are present in the figure legend, table legend, main text, or Methods section.

n/a	Confirmed	
☐	☒	The exact sample size (*n*) for each experimental group/condition, given as a discrete number and unit of measurement
☐	☒	A statement on whether measurements were taken from distinct samples or whether the same sample was measured repeatedly
☐	☒	The statistical test(s) used AND whether they are one- or two-sided *Only common tests should be described solely by name; describe more complex techniques in the Methods section.*
☒	☐	A description of all covariates tested
☒	☐	A description of any assumptions or corrections, such as tests of normality and adjustment for multiple comparisons
☐	☒	A full description of the statistical parameters including central tendency (e.g. means) or other basic estimates (e.g. regression coefficient) AND variation (e.g. standard deviation) or associated estimates of uncertainty (e.g. confidence intervals)
☐	☒	For null hypothesis testing, the test statistic (e.g. *F*, *t*, *r*) with confidence intervals, effect sizes, degrees of freedom and *P* value noted *Give P values as exact values whenever suitable.*
☒	☐	For Bayesian analysis, information on the choice of priors and Markov chain Monte Carlo settings
☒	☐	For hierarchical and complex designs, identification of the appropriate level for tests and full reporting of outcomes
☒	☐	Estimates of effect sizes (e.g. Cohen's *d*, Pearson's *r*), indicating how they were calculated

Our web collection on statistics for biologists contains articles on many of the points above.

Software and code

Policy information about availability of computer code

Data collection	Proteomic mass spectrometry (MS) data was acquired using Xcalibur. link (v.4.0.27.19, Thermo Fisher Scientific) .
Data analysis	Proteomic mass spectrometry raw data were analyzed by MaxQuant (v.1.5.5.1) and Skyline daily. ITC data were analyzed by Origin (v.7.0, OriginLab), data displayed in graphs were analyzed by GraphPad Prism (v.8.0, GraphPadSoftware Inc). Docking were analyzed by AutoDock (v.1.5.6). RNA-seq libraries were analyzed by Bowtie (v.2.2.6), RNA-seq data were analyzed by DESeq2 (v.3.10).

For manuscripts utilizing custom algorithms or software that are central to the research but not yet described in published literature, software must be made available to editors and reviewers. We strongly encourage code deposition in a community repository (e.g. GitHub). See the Nature Research guidelines for submitting code & software for further information.

Data

Policy information about availability of data

All manuscripts must include a data availability statement. This statement should provide the following information, where applicable:

- Accession codes, unique identifiers, or web links for publicly available datasets
- A list of figures that have associated raw data
- A description of any restrictions on data availability

All data needed to evaluate the conclusions in the paper are present in the paper and the Supplementary informations. The MS proteomics data have been deposited to the ProteomeXchange Consortium (http://proteomecentral. proteomexchange.org) via the iProX partner repository with the dataset identifier PXD024897 and PXD024901. The RNA-seq data can be found at the Gene Expression Omnibus database under accession number GSE169499.

Field-specific reporting

Please select the one below that is the best fit for your research. If you are not sure, read the appropriate sections before making your selection.

☒ Life sciences ☐ Behavioural & social sciences ☐ Ecological, evolutionary & environmental sciences

For a reference copy of the document with all sections, see nature.com/documents/nr-reporting-summary-flat.pdf

Life sciences study design

All studies must disclose on these points even when the disclosure is negative.

Sample size	Sample sizes were not predetermined. We used E. coli as research sample.
Data exclusions	No data were excluded.
Replication	All experiments were successfully replicated at least three independent biological experiments, except SILAC MS was performed once. We strictly controlled the labeling efficiency of isotopes above 98% in SILAC MS experiment and checked the data accuracy by synthetic peptides MS analysis, parallel reaction monitoring MS assay and biological verification of key Khib sites.
Randomization	No randomization was necessary as only single variables changed per experiment.
Blinding	Not applicable. Any phenotypic assessment or other measurements was performed using discrete, quantitative measurements.

Reporting for specific materials, systems and methods

We require information from authors about some types of materials, experimental systems and methods used in many studies. Here, indicate whether each material, system or method listed is relevant to your study. If you are not sure if a list item applies to your research, read the appropriate section before selecting a response.

Materials & experimental systems

n/a	Involved in the study
☐	☒ Antibodies
☒	☐ Eukaryotic cell lines
☒	☐ Palaeontology and archaeology
☒	☐ Animals and other organisms
☒	☐ Human research participants
☒	☐ Clinical data
☒	☐ Dual use research of concern

Methods

n/a	Involved in the study
☒	☐ ChIP-seq
☒	☐ Flow cytometry
☒	☐ MRI-based neuroimaging

Antibodies

Antibodies used	Following antibodies were used in this study: Mouse pan anti-2-hydroxyisobutyryllysine monoclonal antibody (pan anti-Khib), PTM Biolabs, Cat# PTM-802, 1:1000 (WB). Rabbit pan anti-acetyllysine monoclonal antibody (pan anti-Kac), PTM Biolabs, Cat# PTM-105RM, 1:1000 (WB). 6×His tag antibody (His. H8), Thermo Fisher Scientific, Cat# MA1-21315, 1:1000 (WB).
Validation	Manufacturer validation: Pan anti-Khib (PTM-802): Species: all; Application: Western blot, Immunoprecipitation; Manufacturer's web site: https://www.ptmbiolabs.com/product/ptm-802/ Pan anti-Kac (PTM-105RM): Species: all; Application: Western blot, Immunoprecipitation; Manufacturer's web site: https://www.ptmbiolabs.com/product/ptm-105rm/ 6×His tag antibody (MA1-21315): Species: Tag; Application: Western blot, Immunoprecipitation; Manufacturer's web site: https://www.thermofisher.cn/cn/zh/antibody/product/6x-His-Tag-Antibody-clone-HIS-H8-Monoclonal/MA1-21315